EUROPEAN COMMISSION

Community research

BELBaR

(Contract Number: 295487)

DELIVERABLE (D-N°: D3.10)

Mechanistic model of radionuclide colloid interaction

Nick Bryan

The National Nuclear Laboratory and The University of Manchester

Reporting period: **01/03/12 – 29/02/16**

Date of issue of this report: **29/02/2016**

Start date of project: **01/03/12** Duration: **48 Months**

Project co-funded by the European Commission under the Seventh Euratom Framework Programme for Nuclear Research &Training Activities (2007-2011)		
Dissemination Level		
PU	Public	X
RE	Restricted to a group specified by the partners of the BELBaR project	
CO	Confidential, only for partners of the BELBaR project	

EURATOM

DISTRIBUTION LIST

Name	Number of copies	Comments
Christophe Davies (EC) BELBaR participants		

1 Introduction

This report describes the advances made in the BELBaR project in the understanding of the interaction between radionuclides and bentonite colloids. It brings together the learning from all of the BELBaR partners.

The report starts with a short description of the issues surrounding colloidal transport and the importance of the reversibility of the interaction between radionuclides and the colloid in determining radionuclide transport. There follows a short description of the experimental data that has been provided during the BELBaR project, and a discussion of the most appropriate rate constants to use in transport calculations. This is followed by a discussion of the possible origins of the slow dissociation that is observed for radionuclides and bentonite colloids. Next there is a description of a mechanistic approach to the treatment of radionuclide colloid kinetics in the safety case of a Geological Disposal Facility (GDF) and estimates of the likely mobility of radionuclides are given based on the currently available knowledge.

1.1 The role of colloids in radionuclide transport

The effect of any colloid (including bentonite) in aiding the transportation of radionuclides depends on a number of factors (Mori et al 2003). For colloidal transport to be important, the following criteria must be met (Mori et al 2003; Missana et al 2008; Honeyman 1999; Miller et al 1994; Ryan and Elimelech 1996):

- **Are colloids present?** - If colloids are not present in the system, then they will not be able to promote radionuclide mobility, but if they are, then they may.

- **Are the colloids mobile?** – If the colloids themselves are not mobile, then they will not be able to promote radionuclide mobility.

- **Are the colloids stable?** - If the colloids are unstable, then any associated radionuclides would be removed from the mobile phase (the solution) as the colloids are destabilised.

- **Is there radionuclide uptake?** – If radionuclides do not bind to the colloids at all, then the colloids cannot promote transport.

Beyond these factors, the nature of the interaction of the radionuclide with the colloid is crucial, and in particular its reversibility. This is the subject of this report.

For the purposes of the following discussion, we can assume that colloid may bind radionuclides in one of two ways: *exchangeably* or *non-exchangeably*. In both modes it can be very strongly bound, but in the exchangeable, it is available for instantaneous release if it encounters a stronger sink, such as the binding sites on a rock surface. In the non-exchangeable state, its release from the colloid is kinetically hindered, and regardless of the strength of the competing sink, time will be required before the radionuclide is released from its host colloid. In the extreme, the radionuclide might be '(pseudo-)irreversibly' bound.

Non-exchangeable binding is required for colloid mediated radionuclide transport to be significant. Figure 1 shows the mechanism for the transport of non-exchangeably bound radionuclides. If colloids encounter radionuclides in a contaminated region, for example in or near a GDF, then they could become bound to the colloid, either exchangeably or non-exchangeably. The colloid could then carry those bound radionuclides with it, for example

a bentonite colloid transporting through a fracture. However, it is expected that any radionuclides that are bound exchangeably, and so may dissociate instantaneously, would be quickly and easily removed by the available rock surface binding sites that will be present in excess. For non-exchangeably bound radionuclides, the strength of the competing sink will not remove the radionuclides, and the radionuclide will be transported with the colloids.

The challenge addressed in the BELBaR project has been to what extent that transport will take place, and how to predict it.

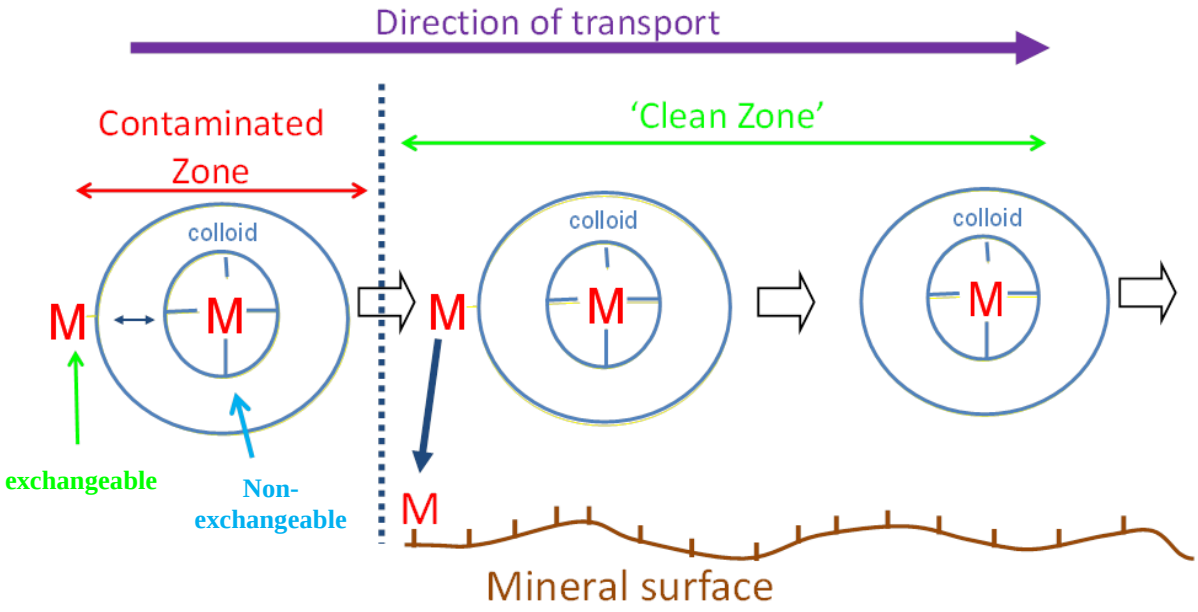

Figure 1*: The mechanism for the transport of radionuclides (M).*

2 Radionuclide Dissociation Rate Constants

The value of the radionuclide dissociation rate constant controls the transport behaviour of the radionuclide. The impact of the rate rate constant will be described below, but given its central role in controlling migration, it is useful to record the dissociation rate constants (k_b) that are now available in one place.

2.1 Experimental Studies

Prior to the start of the BELBaR project, a small number of dissociation rate constants for bentonite colloids were available. Huber et al (2011) determined some dissociation rate constants: for Am(III), the values are in the range 0.0037 - 0.009 hr^{-1} (1 - 2.5 $x10^{-6}$ s^{-1}), whilst for Pu(IV), the range is 0.0014 - 0.0085 hr^{-1} (3.9 $x10^{-7}$ - 2.4 $x10^{-6}$ s^{-1}). In lab column experiments, Missana et al. (2008) studied Eu(III) transport by bentonite colloids. Taking into account the residence time, the percentage recovery of the colloids and the amount of Eu that was associated with the colloids, it is possible to estimate an overall apparent first order dissociation rate constant of 4.8×10^{-4} s^{-1} for the experiment. Pu(IV) experiments by the same authors, showed slower dissociation of Pu, with no significant dissociation within the column. Under these circumstances, it is not possible to estimate a definitive dissociation rate constant for Pu(IV), but it is possible to estimate an upper limit (>10^{-5} s^{-1}). Dissociation data are difficult and time consuming to produce. Therefore, Wold (2010) estimated first order dissociation rate constants (k_b) for: Pu(IV) 4.35$x10^{-3}$ hr^{-1} (= 1.2$x10^{-6}$ s^{-1}); Am(III) 2$x10^{-3}$ hr^{-1} (= 5.6$x10^{-7}$ s^{-1}); Np(IV) 4.6$x10^{-7}$ hr^{-1} (= 1.2$x10^{-10}$ s^{-1}); Cm(III) 6$x10^{-3}$ hr^{-1} (= 1.7$x10^{-6}$ s^{-1}); U(VI) 3$x10^{-3}$ hr^{-1} (= 8.3$x10^{-7}$ s^{-1}); Tc(IV) 0.63 - 15 hr^{-1} (= 1.75$x10^{-4}$ - 4.2$x10^{-3}$ s^{-1}). However, these values were estimated from sorption rate constants (k_f) and assuming that $K_d = k_f/k_b$. For a simple (single) chemical reaction, this will be true, but for a more complex process, then the dissociation constant may not behave in this way.

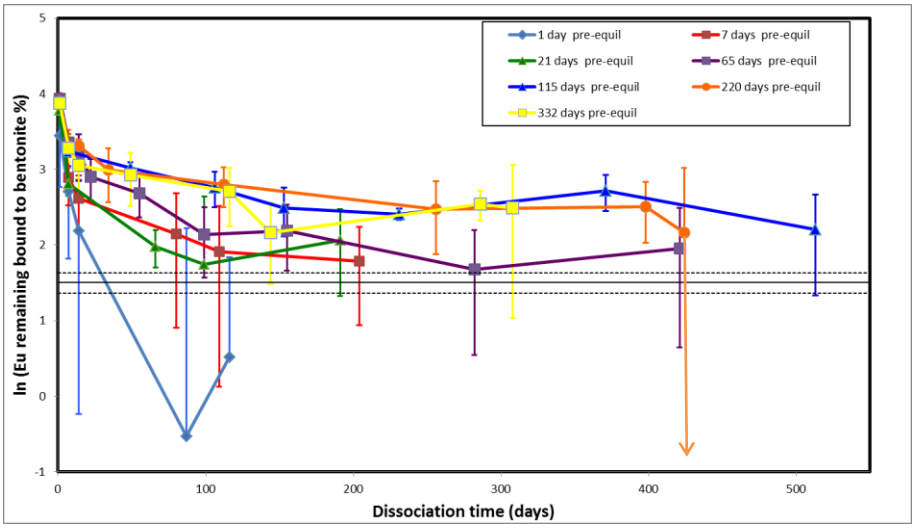

Figure 2*: Natural log of percentage of Eu bound to bentonite vs EDTA contact time, as a function of pre-equilibration time (pH = 7 ± 0.1; I = 0.1 M $NaClO_4$). The full black horizontal line represents the equilibrium position, and the dashed lines represent the experimental uncertainty for the equilibrium position. Errors bars are 2σ based on the standard deviation of triplicate measurements.*

During BELBaR, the dissociation of radionuclides from bulk bentonite was measured using competition from EDTA to 'pull' the radionuclide ions from the clay and into solution (Sherriff et al 2015). Figure 2 shows the dissociation of Eu(III) from bentonite with EDTA contact time as a function of pre-equilibration time of the Eu with the bentonite prior to addition of EDTA. A large part of the Eu(III) (30 - 50 %) dissociated

almost instantaneously from the clay. For the experiments with pre-equilibration times less than 115 days, the Eu distribution between bulk bentonite and EDTA was within error of that at equilibrium between 20 and 100 days. Experiments with pre-equilibration times above 115 days took longer to reach the equilibrium distribution, but all of them were tending towards equilibrium. Therefore, there was no convincing evidence for irreversibility. For pre-equilibration times less than 1 week the dissociation was distinctly faster. The average dissociation rate constant for this system (taken from day 1 of EDTA contact until the system reaches apparent equilibrium) is approximately 10^{-6} s^{-1}. For pre-equilibration times ≥ 1 week, there is evidence for more than one dissociation rate constant. The first order dissociation rate constants for the slowest observed component and the amounts in that component are given in Table 1. There are relatively small differences between the rates for the different systems. The average Eu(III) dissociation rate constant is 4.3×10^{-8} s^{-1}, with a range of 2.2×10^{-8} – 1.0×10^{-7} s^{-1}. Further, this fraction corresponds to a significant amount of the bentonite bound radionuclide, typically 20%.

Table 1: ***Dissociation rate constants, reaction half time data and amounts for the most slowly dissociating fraction for Eu and bulk bentonite (pH = 7 ± 0.1; I = 0.1 M $NaClO_4$). Errors are 2σ based on the error determined during regression of the data.***

Pre-equilibration Time/day	Dissociation rate constant (s^{-1})	Amount of Eu in slow dissociating fraction with errors (%)	τ (Days)
7	1.01×10^{-7} ($\pm 6.23 \times 10^{-8}$)	17.3 (+3.1; -2.9)	79
21	4.19×10^{-8} ($\pm 8.51 \times 10^{-8}$)	11.9 (+25.2; -4.8)	192
65	3.93×10^{-8} ($\pm 1.35 \times 10^{-8}$)	19.3 (+5.4; -3.5)	204
115	2.17×10^{-8} ($\pm 1.70 \times 10^{-8}$)	20.5 (+8.6; -6.0)	370
220	2.61×10^{-8} ($\pm 1.14 \times 10^{-8}$)	24.3 (+6.7; -5.2)	308
332	2.56×10^{-8} ($\pm 2.87 \times 10^{-8}$)	20.7 (+11.2; -7.3)	314

Sherriff et al (2015) also studied the dissociation of Eu from bentonite colloids. Figure 3 shows the dissociation of Eu(III) from the bentonite colloids as a function of Eu/colloid pre-equilibration time. In this system, cation exchange resin was used to remove the radionuclide from the colloids. For all experiments, a similar pattern is observed. A significant part of the radionuclide (approximately 30 - 40 %) dissociated almost instantaneously. This was followed by slower dissociation over time, but that dissociation was very different to that of the bulk bentonite:

- More radionuclide is found in the slowly dissociating fraction;
- There is no increase in the amount bound beyond 1 day pre-equilibration time;
- Beyond the initial rapid dissociation, only a **single** rate constant is observed.

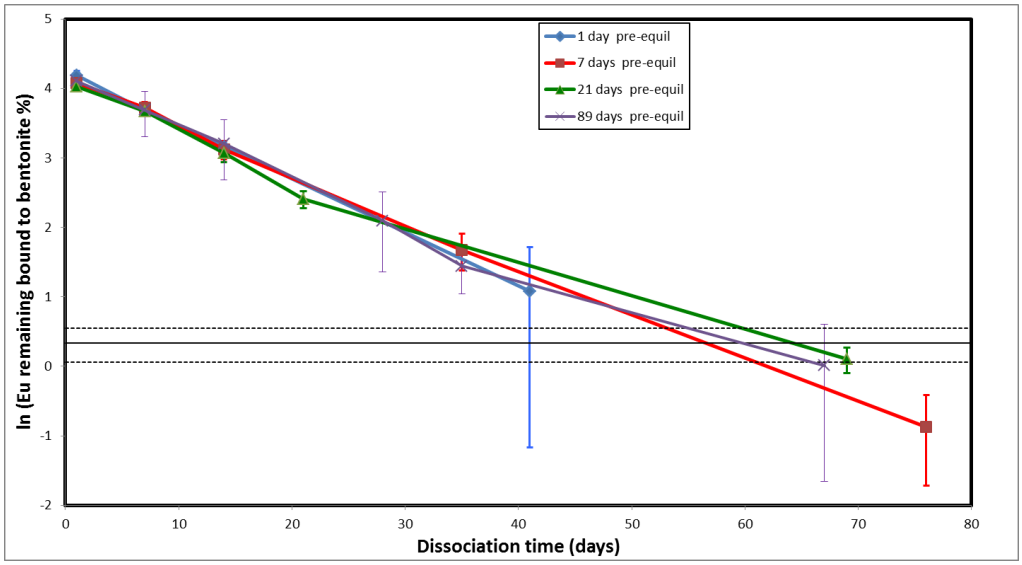

Figure 3*: Natural log plot of the colloid dissociation experiment: ln(percentage bound to bentonite) vs Dowex resin contact times, as a function of pre-equilibration time (pH = 8.8 ± 0.1). The black horizontal line represents the equilibrium distribution, and the dashed lines represent the experimental uncertainty.*

The first order dissociation rate constants and the amounts in the most slowly dissociating component were calculated by regression, and the results are shown in Table 2.

Table 2*: Dissociation rate constants, reaction half time data and amounts for the most slowly dissociating fraction (pH = 8.8 ± 0.1). Note, calculating an overall rate for all data gives an average first order rate constant of 8.8 x 10^{-7} s^{-1}. Errors are 2σ based on the error determined during regression of the data.*

Pre-equilibration System/day	Dissociation rate constant (s^{-1})	Amount of Eu in fraction (%)	τ (Days)
1	8.97 x 10^{-7} (±2.27 x 10^{-8})	69.8 (+3.1; -2.9)	8.94
7	7.66 x 10^{-7} (±5.63 x 10^{-8})	60.8 (+12.4; -10.3)	10.5
21	9.47 x 10^{-7} (±2.63 x 10^{-7})	64.9 (+22; -17)	8.47
89	9.04 x 10^{-7} (±2.55 x 10^{-8})	69.2 (+11; -9.5)	8.87

Therefore, the dissociation rate constants for the colloids are over an order of magnitude higher than for the bulk. The reasons for the differences are uncertain, but it could be due to the narrow size distribution of the bentonite colloids. Beyond being more heterogeneous in terms of particle size, as a natural material, the bulk sample is also more chemically heterogeneous too. It seems likely that both of these factors contribute to the difference.

Sherriff et al (2015b) measured the dissociation of uranium from bentonite colloids in systems where the uranium had been added to the system as U(VI). Figure 4 shows the dissociation of uranyl from bentonite colloids as a function of U/colloid pre-equilibration time. There are some differences between the uranyl and Eu experiments. The first is that in the uranium system, the intrinsic interaction is much weaker, and it was found that only

half (54%) of the uranium bound to the colloids. However despite that, the uranium that did dissociate did show slow dissociation.

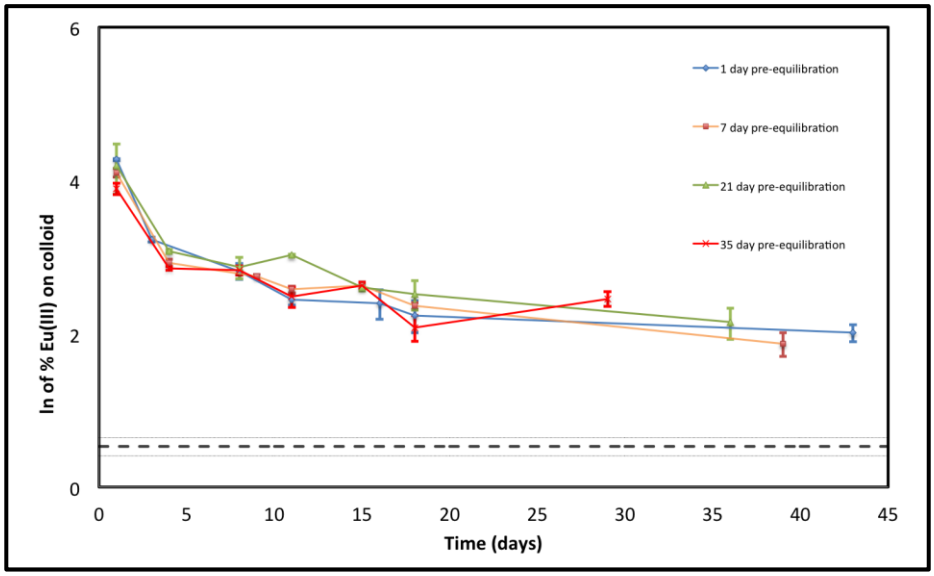

Figure 4*: Natural log plot of the colloid dissociation experiment: ln(percentage ([U] = 5.43 x 10^{-10} M) bound to bentonite) vs time (days), pH = 8.8 ± 0.2. The dashed black horizontal line represents the equilibrium distribution.*

On first contact with the Dowex resin, there is an instantaneous reduction in the amount of U in solution (approximately 30-50 %). Given that 46 % of the uranium in the solution is not colloid associated, much of this material must be that component. The data suggest that there is a fraction accounting for approximately 30% of the material that corresponds to material that is not released instantaneously, but that shows faster dissociation that the slowest fraction. The first order dissociation rate constants and the amounts are given in Table 3. The average dissociation rate constant is 5.6×10^{-7} s^{-1} ($\pm 4.2 \times 10^{-7}$).

Table 3*: Dissociation rate constants, reaction half time (τ) data and amounts for the most slowly dissociating fraction (pH = 8.8 ± 0.1). Note, calculating an overall rate for all data gives an average first order rate constant of 5.6 x 10^{-7} s^{-1}. Errors are 2σ based on the error determined during regression of the data.*

Pre-equilibration System/day	Dissociation rate constant (s^{-1})	Amount of U in fraction (%)	τ (Days)
1	7.8×10^{-7} ($\pm 5.8 \times 10^{-7}$)	27.9 (+24.3; -13.0)	11
7	3.1×10^{-7} ($\pm 1.6 \times 10^{-6}$)	20.4 (+69.7; -15.8)	25.8
21	4.6×10^{-7} ($\pm 2.4 \times 10^{-7}$)	24.9 (+7.2; -5.6)	17.4
35	6.9×10^{-7} ($\pm 9.0 \times 10^{-7}$)	23.7 (+33.8; -14.0)	11.7

Huber et al (2015) studied the dissociation of tri and tetravalent actinides from montmorillonite colloids that had been labelled with either Zn or Ni. They used batch experiments with dissociation times of 10,000 hours. For Am(III), they found that both colloid types gave the same first order dissociation rate constant (3.4 x 10^{-7} s^{-1}), whilst for

Pu(IV) the constants were 7.7 x 10^{-8} s^{-1} and 3.4 x 10^{-7} s^{-1} for the Zn and Ni labelled species, respectively. For Th(IV), there was a larger difference between the values for the two colloids, with rate constants of 9.4 x 10^{-10} s^{-1} and 2.6 x 10^{-7} s^{-1} for the Zn and Ni labelled species, respectively. The value for the Zn labelled colloids is much lower than any of the other experimentally determined values. However, the authors cautioned strongly against over-interpretation of the rate constant values for Th given the scatter in the experimental data.

Dittrich et al (2015) determined Am(III) dissociation rate constants from laboratory column experiments, where the Am solution was passed through sequential columns of fracture filling material. They found that the Am behaved with the same rate constant for the columns, which was interpreted as evidence that the Am was dissociating with a single rate constant. The rate constants were of the order of 2.5 – 2.7 x10^{-5} s^{-1}, for column experiments with residence times of approximately 6 hours. The constants were determined using a coupled chemical transport model that assumed a single binding mode for all bentonite associated colloid.

Bentonite colloid and radionuclide migration experiments have taken place at the Grimsel test site in Switzerland as part of the Colloids Formation and Migration project (CFM). In these experiments, mixtures of radionuclides and bentonite colloids have been injected into a saturated shear zone in a fractured granodiorite formation. Following transport, the solution was captured and the radionuclide concentration determined. Wang et al (2014) modelled tri and tetra-valent breakthrough curves from these experiments. They applied a number of conceptual models:

1. All ions bound at a single site, with a single first order dissociation rate constant;

2. Two radionuclide binding sites, each with its own first order dissociation rate constant;

3. A single binding site that shows first order dissociation, but with an ageing term that has the effect of reducing the rate constant with time;

4. Two radionuclide binding sites, each with its own first order dissociation rate constant and with first order transfer between the two sites and with all ions initially bound at a single site.

5. Two radionuclide binding sites, each with its own first order dissociation rate constant and with first order transfer between the two sites, but with an adjustable initial distribution of ions between the two sites.

They found that the model approach that gave the best fit to the different experimental data sets varied from one system to another. For some of the best fits, the parameters were unexpected, for example transfer with time to a second site with faster dissociation. Some of the best fits were obtained by setting the second site dissociation rate constant to zero, i.e., irreversible binding, although the experiments showed no direct conclusive evidence for irreversible binding.

The best fit first order dissociation rate constants for the CFM data using the single site modelling approach (1) are given in Table 4.

Table 4: ***first order dissociation rate constants derived by fitting radionuclide breakthrough data from experiments at the Grimsel site (CFM project). Data from Wang et al (2014).***

	Dissociation rate constant k_b (s^{-1})	**Residence time (hour)**	**CFM run**	**Best fit model approach**
Th(IV)	3.78×10^{-6}	3.6	08-01/Th	1
Hf(IV)	2.25×10^{-5}	3.6	08-01/Hf	1
Th(IV)	7.03×10^{-6}	22	10-01/Th	4
Hf(IV)	1.02×10^{-5}	22	10-01/Hf	1
Th(IV)	8.33×10^{-7}	60	10-03/Th	5
Hf(IV)	5.83×10^{-7}	60	10-03/Hf	4
Pu(IV)	2.14×10^{-6}	34	12-02/Pu	4
Tb(III)	5.33×10^{-5}	3.6	08-01/Tb	1
Tb(III)	2.06×10^{-5}	22	10-01/Tb	4
Eu(III)	2.39×10^{-5}	22	10-01/Eu	2
Tb(III)	1.15×10^{-5}	60	10-03/Tb	2
Eu(III)	7.22×10^{-6}	60	10-03/Eu	5
Am(III)	4.53×10^{-6}	34	12-02/Am	1

2.2 Analysis of rate constant data for the safety case

Given that the dissociation rate constant plays such a central role in determining the transport of radionuclides, all of the currently available experimental and theoretical values (of which the author is aware) have been collated together in Table 6. The experimental data are shown together in Figure 5, where they have been plotted versus the available reaction time during the measurement. For experiments that used laboratory columns or the Grimsel CFM data, this is the transport residence time, whilst for the batch experiments, it is the time that was available for dissociation to take place.

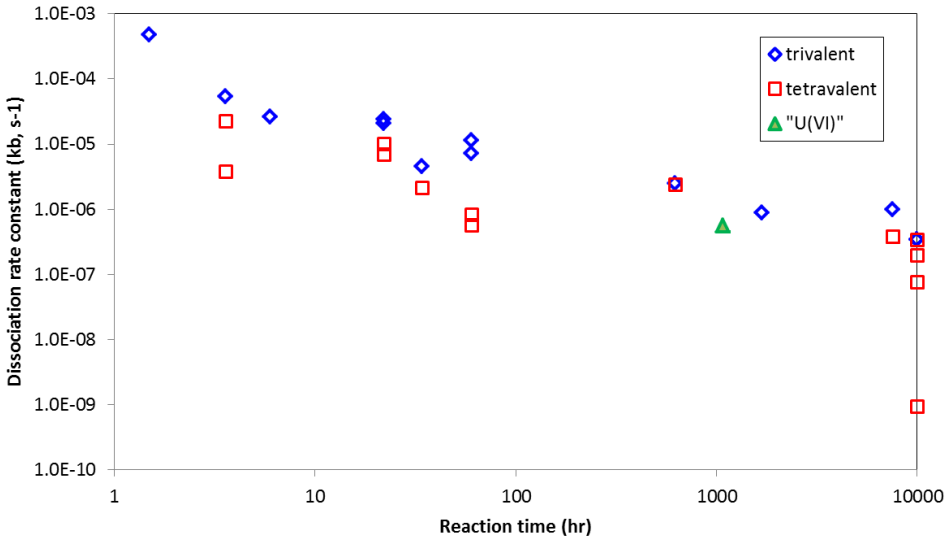

Figure 5: ***All available dissociation rate constants plotted versus the available reaction time during measurement: residence time for columns and CFM data; dissociation times for batch experiments.***

Considering that the data have been determined by different groups for different elements and using such disparate techniques, from simple batch reactions to in situ experiments at the Grimsel site, the correlation between the data is very striking. The data for reaction times less than 100 hours derive from transport experiments (lab columns and Grimsel), whilst those for reaction times greater than 100 hours are from batch experiments. The data show that the same processes are being measured in transport and batch experiments, and that the only difference is the available reaction time. Hence, the values obtained from the batch experiments may be applied in transport calculations.

The data for the trivalents are generally very slightly higher for the transport experiments ($t < 100$ hours) than for the tetravalent, although the scatter in the data means that the ranges overlap. For the batch experiments, it is much harder to detect a significant difference between the two types. There is a clear outlier in the data at a reaction time of 10,000 hours, which is the point for Th(IV) dissociation from Zn-labelled montmorilonite colloids (9.4×10^{-10} s^{-1}) determined by Huber et al (2015). However, the rate constant determined at the same time for the Ni-labelled monmorilonite (2.6×10^{-7} s^{-1}) is in line with the other values. Huber et al (2015) cautioned against overinterpretation of the Th data, due to the scatter of the experimental data and its effect on the fitting process. Given there are a cluster of points at long reaction times with $k_b \approx 10^{-7}$ s^{-1}. It seems likely that these represent a better measure of the dissociation rate constant.

The U data from Sherriff et al (2015b) has been plotted in Figure 5, although in that experiment, the uranium was added to the system as uranyl, the measured dissociation rate constant is in line with the data for the tetravalent ions. This could indicate that the uranyl shows broadly similar dissociation behaviour to the other ions. Alternatively, given that the uranium in that experiment was present at ultra-trace level, due to the use of ^{232}U, it is possible that reduction has taken place, and that the slowly dissociating U is present as U(IV).

The dependence of the apparent rate constant on the reaction time might seem counterintuitive, since the radionuclides will be bound in the same way to the colloids regardless of the method that is used to measure their dissociation. The origin of the effect is probably two-fold.

First, the batch experiments have shown that radionuclides can be bound both exchangeably (relaively quickly released) or non-exchangebly. For example, in the case of the europium data of Sherriff et al (2015), 30 – 40% of the Eu(III) was bound exchangeably and would dissociate within 1 day. In a transport experiment, this material would be removed relatively easily, and then as the colloid progressed, some further fraction would be lost from the non-exchangeable. Therefore, an approach that fits all loss of Eu from the colloid with a single rate constant will tend to overestimate the value.

Secondly, in order to measure a given first order rate constant, the experiment must have sufficient time to allow that process to take place. Taking a system with a rate constant of 10^{-7} s^{-1} in an experiment with a residence time of 100 hours, only approximately 3.5 % of the metal ion will dissociate. Such a small reduction would be difficult to detect, whereas in experiments withreaction times of 1000 and 10,000 hours, the extent of dissociation would be approximately 30% and 97%, respectively. Hence, if radionuclide is dissociating with a rate constant of approximately 10^{-7} s^{-1}, then it would be very difficult to measure that rate accurately with a relatively short residence time transport experiment. This shows the advantage of combining data from batch and transport experiments.

The data in Figure 5 cover reaction times (and hence transport residence times) up to 10,000 hours (400 days), and so for situations with transport residence times in this range, the experimental data may be used directly. However, there is a question of the appropriate constant for longer residence times. The data in the figure were fitted, and it was found that fits using power law equations gave by far the best match to the data. Separate fits were performed using:

1. the trivalent data only;

2. the tetravalent data only, exluding the outlying point for Th(IV) and Zn-labelled monmorilonite;

3. all data, including the 'U(VI)' data from Sherriff et al (2015b), but still excluding theTh(IV) outlier

The results are shown in Figure 6. The best fit equations and correlation coefficients were:

Trivalent data	$\mathbf{k_b = 1.51 \times 10^{-4}.(t^{-0.656})}$	$\mathbf{R^2 = 0.911}$
Tetravalent data	$\mathbf{k_b = 1.52 \times 10^{-5}.(t^{-0.454})}$	$\mathbf{R^2 = 0.734}$
All data	$\mathbf{k_b = 5.61 \times 10^{-5}.(t^{-0.582})}$	$\mathbf{R^2 = 0.756}$

Note: given that these are best fit equations for first order rate constants expressed in s^{-1} and reaction times in hours, and given the likely origin of the variation in rate constant with reaction time, no mechanistic significance should inferred from the values of the parameters in the equations.

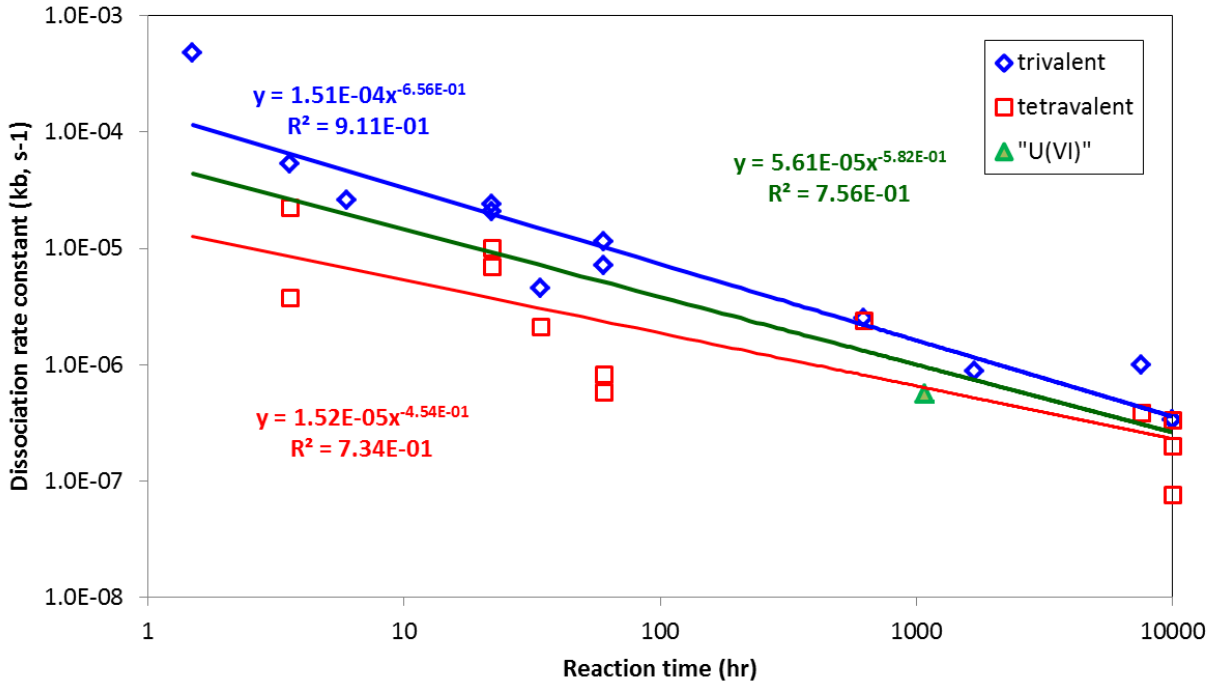

Figure 6: ***fitting of dissociation rate constant data: red = fit to tetravalent data only; blue = fit to trivalent only; green = fit to all data combined.***

The equations may be used to make forecasts of the rate constants, **assuming that there are no other significant processes in the system that were not evident in the experiments**. Figure 7 shows extrapolations of the three fitting equations to 10^7 hours (1,140 years). Selected values for each of the fits are given in Table 5.

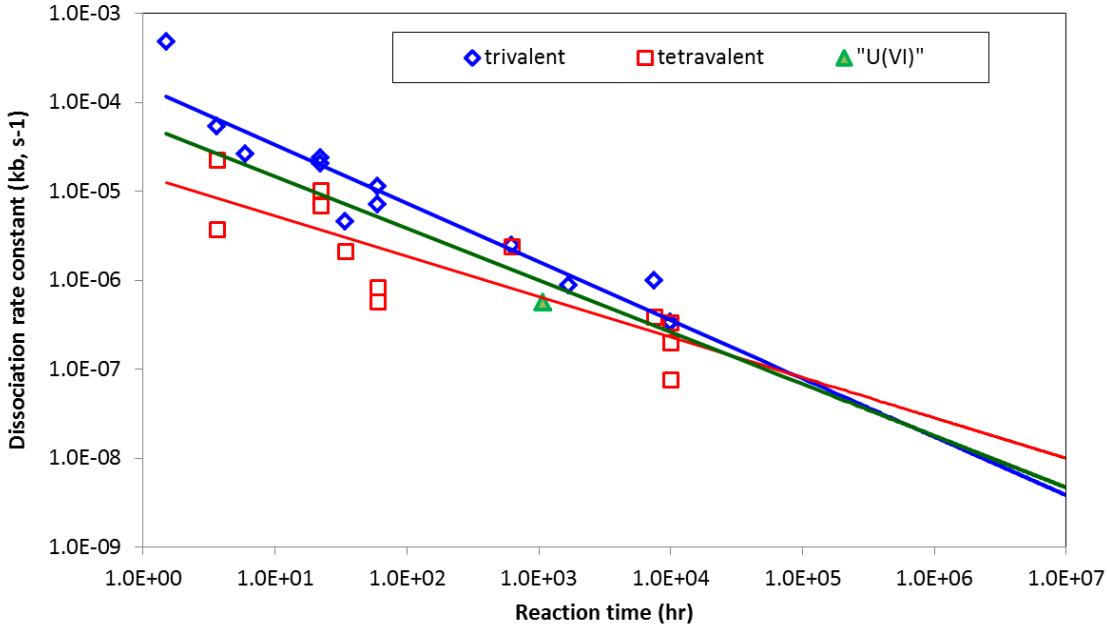

Figure 7: ***forecast of first order dissociation rate constants up to reaction (residence) times of 10^7 hours***

Table 5: ***forecasted values of the first order dissociation constant***

Residence time (hr)	Residence time (year)	Trivalent (s^{-1})	Tetravalent (s^{-1})	All data (s^{-1})
10000	1.1	3.6×10^{-7}	2.3×10^{-7}	2.6×10^{-7}
50000	5.7	1.2×10^{-7}	1.1×10^{-7}	1.0×10^{-7}
100000	11	7.9×10^{-8}	8.2×10^{-8}	6.9×10^{-8}
500000	57	2.8×10^{-8}	3.9×10^{-8}	2.7×10^{-8}
1000000	114	1.7×10^{-8}	2.9×10^{-8}	1.8×10^{-8}
5000000	570	6.1×10^{-9}	1.4×10^{-8}	7.1×10^{-9}
10000000	1141	3.9×10^{-9}	1.0×10^{-8}	4.7×10^{-9}

Safety case calculations are often made over very long time periods, sometimes hundreds of thousands of years. In that case, the fact that the fits have only been extrapolated to 10^3 years might seem odd. However, the residence times plotted in Figure 7 should not be confused with the total calculation times. The residence times are equivalent to those that would be taken for a radionuclide attached to a colloid to travel across the flow path being considered in a calculation. In that sense, a residence time of 10^3 years is relatively long. For example, a residence time of 10^3 years over a total ditance of 100 m represents a flow rate of approximately 3×10^{-9} ms^{-1}, and even over a distance of 1 km, the flow rate would be 3×10^{-8} ms^{-1}.

Caution is required when applying the extrapolated rate constants given in Figure 7 and **Error! Reference source not found.**. All of the experimental data only cover residence times up to approximately 1 year, and these are being extrapolated well outside of their range. As such, they represent an interesting prediction, but it is possible that there are effects that they do not capture. The extrapolations appear to suggest that the trivalents might show slower dissociation than the tetravalents for very long residence times. However, this is certainly an artefact of the fitting and the larger scatter in the tetravalent experimental data. There is nothing in the experimental data to suggest that this is a real difference. As such, the values given by the three extrapolations represent together the ranges of values that the current data suggest might be observed and nothing more.

Beyond the uncertainty in the data fitting, there is also the issue that in order to detect and measure kinetic effects, experiments must have a reaction time comparable to the reaction half-time. Hence, in the same way that an experiment with a residence time of 100 hours, will struggle to measure or detect a rate constant of 10^{-7} s^{-1}, an experiment with a reaction time of 10,000 hours will not detect dissociation with a rate constant of 10^{-9} s^{-1}. Hence, it cannot be excluded that there is some small fraction of the bound radionuclide that might dissociate with a rate constant of less than approximately 10^{-9} s^{-1}. Of course, it is also possible that no further decrease in rate constant takes place as residence time increases beyond 1 year, but the data do not demonstrate that.

Table 6: collated radionuclide dissociation rate constant for all experimental and theoretical studies

Ion	Dissociation rate constant (k_b, s^{-1})	Experimental or Theoretical	Details	Residence/ dissociation time (hr)	Reference
Am(III)	2.5×10^{-6}	Experimental	Batch experiment	624	Huber et al 2011
Am(III)	1×10^{-6}	Experimental	Batch experiment	7500	Huber et al 2011
Am(III)	2.6×10^{-5}	Experimental	Laboratory column experiments	6	Dittrich et al 2015
Am(III)	3.4×10^{-7}	Experimental	Batch experiment using Zn labelled montmorillonite colloids	10000	Huber et al 2015
Am(III)	3.4×10^{-7}	Experimental	Batch experiment using Ni labelled montmorillonite colloids.	10000	Huber et al 2015
Am(III)	4.53×10^{-6}	Experimental	CFM experiment	34	Wang et al 2014
Am(III)	5.6×10^{-7}	Theoretical	Calculated from K_d values and association rates	-	Wold 2010
Cm(III)	1.7×10^{-6}	Theoretical	Calculated from K_d values and association rates	-	Wold 2010
Eu(III)	4.8×10^{-4}	Experimental	Laboratory column experiments	≈ 1 -2 hours	Missana et al. 2008
Eu(III)	8.79×10^{-7}	Experimental	Batch experiment	1680	Sherriff et al 2015
Eu(III)	2.39×10^{-5}	Experimental	CFM experiment	22	Wang et al 2014
Eu(III)	7.22×10^{-6}	Experimental	CFM experiment	60	Wang et al 2014
Tb(III)	1.15×10^{-5}	Experimental	CFM experiment	60	Wang et al 2014
Tb(III)	2.06×10^{-5}	Experimental	CFM experiment	22	Wang et al 2014
Tb(III)	5.33×10^{-5}	Experimental	CFM experiment	3.6	Wang et al 2014
Pu(IV)	2.4×10^{-6}	Experimental	Batch experiment	624	Huber et al 2011
Pu(IV)	3.9×10^{-7}	Experimental	Batch experiment	7500	Huber et al 2011
Pu(IV)	$< 10^{-5}$	Experimental	Laboratory column experiments: upper limit estimate	≈ 1 - 2 hours	Missana et al. 2008
Pu(IV)	7.7×10^{-8}	Experimental	Batch experiment using Zn labelled montmorillonite colloids	10000	Huber et al 2015
Pu(IV)	3.4×10^{-7}	Experimental	Batch experiment using Ni labelled montmorillonite colloids.	10000	Huber et al 2015
Pu(IV)	2.14×10^{-6}	Experimental	CFM experiment	34	Wang et al 2014
Pu(IV)	1.2×10^{-6}	Theoretical	Calculated from K_d values and association rates	-	Wold 2010

Ion	Dissociation rate constant (k_b, s^{-1})	Experimental or Theoretical	Details	Residence/ dissociation time (hr)	Reference
Th(IV)	3.9×10^{-7}	Experimental	Batch experiment	7500	Huber et al 2011
Th(IV)	9.4×10^{-10}	Experimental	Batch experiment using Zn labelled montmorillonite colloids	10000	Huber et al 2015
Th(IV)	2.6×10^{-7}	Experimental	Batch experiment using Ni labelled montmorillonite colloids.	10000	Huber et al 2015
Th(IV)	3.78×10^{-6}	Experimental	CFM experiment	3.6	Wang et al 2014
Th(IV)	7.03×10^{-6}	Experimental	CFM experiment	22	Wang et al 2014
Th(IV)	8.33×10^{-7}	Experimental	CFM experiment	60	Wang et al 2014
Np(IV)	1.2×10^{-10}	Theoretical	Calculated from K_d values and association rates		Wold 2010
Hf(IV)	5.83×10^{-7}	Experimental	CFM experiment	60	Wang et al 2014
Hf(IV)	2.25×10^{-5}	Experimental	CFM experiment	3.6	Wang et al 2014
Hf(IV)	1.02×10^{-5}	Experimental	CFM experiment	22	Wang et al 2014
Tc(IV)	1.75×10^{-4} - 4.2×10^{-3}	Theoretical	Calculated from K_d values and association rates		Wold 2010
U(VI)	5.60×10^{-7}	Experimental	Batch experiment	1080	Sherriff et al 2015b
U(VI)	8.3×10^{-7}	Theoretical	Calculated from K_d values and association rates		Wold 2010

3 The Chemical Origin of Slow Dissociation

There are a number of mechanisms that could be responsible for the slow dissociation.

(1) Slow disociation of a surface complex.

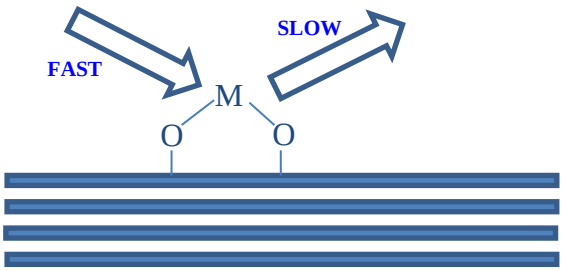

The radionuclides could bind at a surface site from which dissociation is slow. In this case, the dissociation kinetics would be expected to depend upon the radionuclide chemistry. However, there is very little variation in the first order dissociation rate constant from one radionuclide to another. Further, if slow dissociation of surface complexes is responsible, then not all surface complexes show this behaviour, because not all of the radionuclide loading is bound non-exchangeably in all cases.

For hard ions, such as the lanthanides and actinides, we would not automatically expect dissociation from a surface complexation site to be so slow, and indeed this behaviour has not been reported with other inorganic surfaces. Hence, on balance it seems unlikely that this is the origin of the effect, at least on its own.

(2) Slow disociation of a surface precipitate.

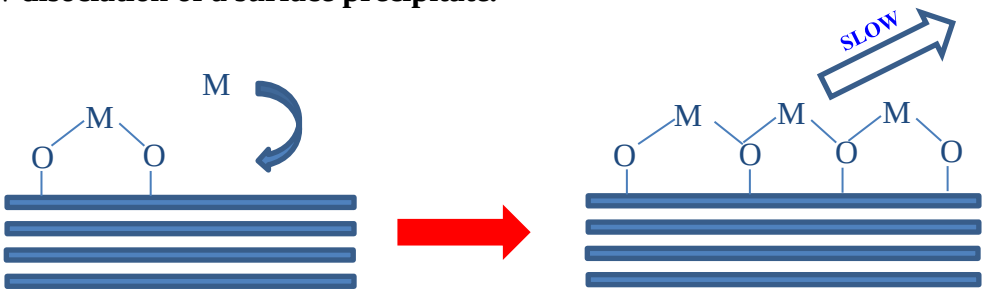

The radionuclides could form a surface precipitate, probably following surface complex formation. Dissolution of this precipitate could be slow, and particularly for the tetravalent actinides (Bouby et al 2011). As for surface complexation, the kinetics might be expected to depend upon radionuclide chemistry. The relatively small differences between the rate constants for the tri and tetravalent actinides are surprising if the origin of the effect is the slow dissolution of a surface precipitate of the radionuclide on its own. Further, any surface precipitation must take place at very low concentration given that slow dissociation has been observed for experiments with very low radionuclide concentrations down to 10^{-10} M (Sherriff et al 2015, 2015b). However, if the radionuclides were being incorporated in some sort of surface layer derived from the clay, then the release could be similar for different ions (as observed).

(3) Diffusion in and out of an interlayer.

Radionuclides could enter the clay interlayer from the solution. When a stronger sink becomes available, the radionuclides could then diffuse slowly from the interlayer, resulting in the observed slow dissociation.

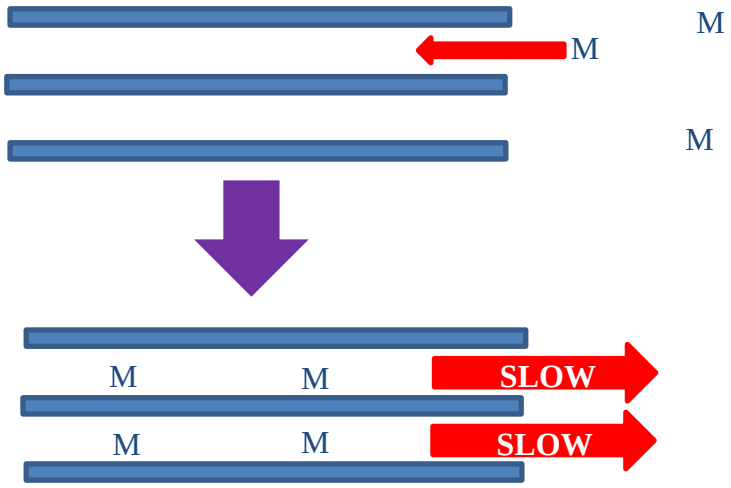

The process responsible for the non-exchangeable effect seems to be particular to bentonite and montmorillonite colloids. Therefore, it is certainly possible that it is some property of clays that is responsible for the effect. The presence of the interlayer is such a property.

Estimating the diffusion of radionuclides into the interlayer of a single colloid would require the correct interlayer diffusion coefficient for a colloid. However, one of the behaviours that any process would have to explain is the similarity in the behaviour for all of the trivalent and tetravalent ions. Brandberg and Skagius (1991) proposed effective diffusivities for bulk bentonite: they recommended the same value for the tri and tetravalent ions. Hence, it is possible that they might show similar behaviour in the colloidal interlayer.

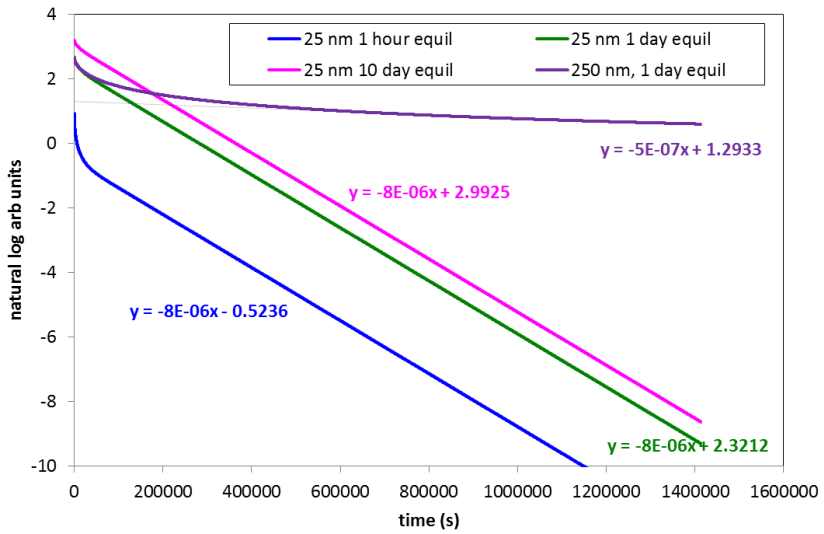

Figure 8: ***simulations of dissociation for a 1-D diffusion process.***

Figure 8 shows simulations of the dissociation behaviour that might be observed for simple diffusion into a 1-D channel representing the interlayer during pre-equilibration followed by slow diffusion out of the channel during dissociation. By selecting the correct arbitrary

diffusion coefficient, it is possible to generate data that appears broadly similar to that observed in the dissociation experiments. However, the behaviour is sensitive to the size of the channel. Also, although portions of the plots have gradients that are similar to those measured in batch dissociation experiments, the behaviour is not always consistent with a single rate constant. Hence, there are aspects of the behaviour that could be consistent with interlayer diffusion, although it is by no means certain.

(4) Colloid aggregation.

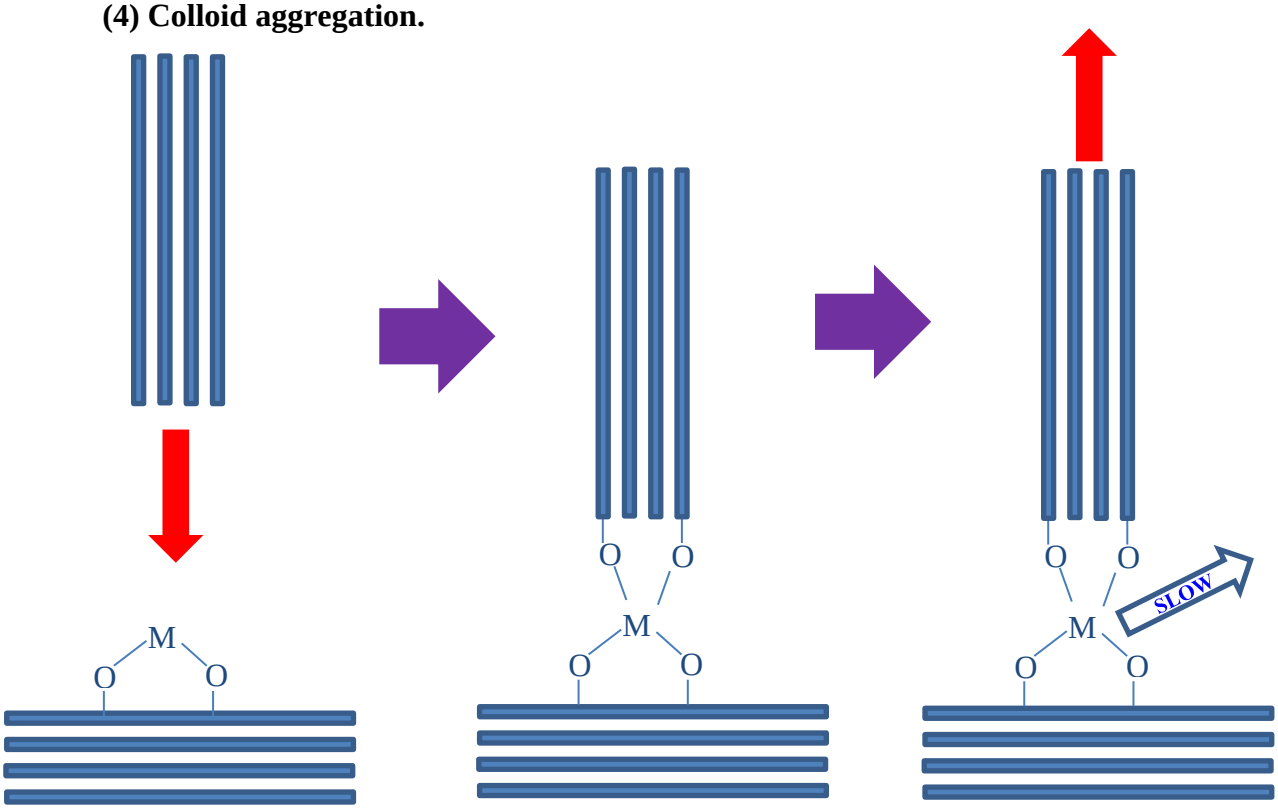

A radionuclide could be bound to a clay colloid in a state that is initially exchangeable. However, colloidal aggregation could 'trap' the radionuclide in a state where it is 'hidden' from the solution and unavailable for instantaneous reaction. The release from this state could be slow, and might require the dissociation of the aggregate.

This mechanism could explain slow dissociation from clay colloids, and it cannot be ruled out that it could play some role in the process, although the aggregation and dissociation rates would be expected to depend upon the colloid concentration, and this has not been observed. The Eu data from Sherriff et al (2015) show that the majority of the radionuclide loading shows slow dissociation. Further, the reaction is largely complete within one day. If the radionuclides were being trapped (and then released) by the aggregation/disaggregation processes that the clay colloids show ordinarily, then this behaviour would not expected. If this process is responsible, then it seems likely that the presence of the radionuclide ion is affecting the interaction in some way, perhaps by promoting aggregation. This could explain why such large fractions of the radionuclides can become bound non-exchangeably. The knowledge of the interactions between radionuclides and bentonite colloids is insufficient to allow any quantitative analysis of this reaction.

(5) Binding by associated organic material.

A radionuclide could be bound by organic material that is associated with the clay. Humic substances are known to show slow radionuclide dissociation, and so if a radionuclide bound to a humic molecule associated with a clay colloid, then slow dissociation would be expected.

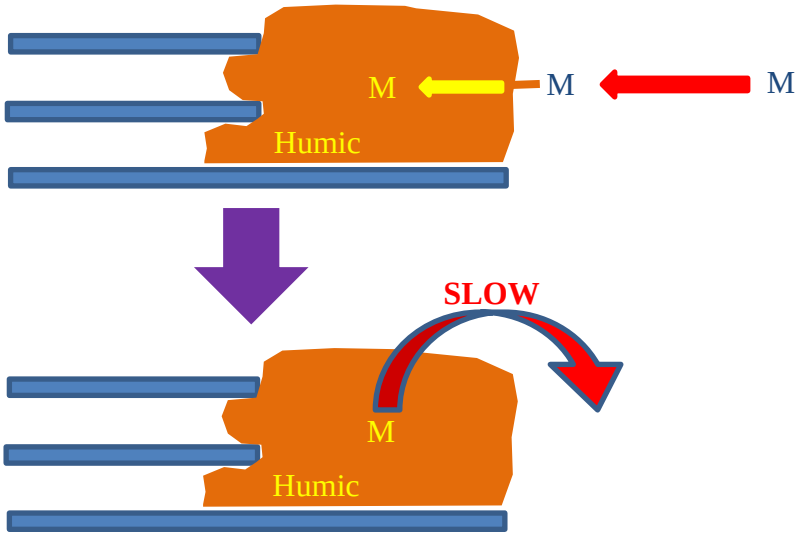

Interestingly, the first order rate constants that are found for humic substances under conditions of low humic substance concentration are of the order of $1 – 5 \times 10^{-7}$ s^{-1}, and this is the approximate magnitude of the rate constants that have been observed for radionuclide interactions with bentonite colloids. There is evidence for the complexation of metal ions by organic material naturally present in bentonite (e.g. Geckeis et al 2004), and so it is tempting to associate the slow kinetics with entrained natural organic material. However, the Zn and Ni labelled colloids studied by Huber et al (2015) where synthesised in the laboratory from laboratory reagents, and yet their dissociation rate constants are entirely in line with those derived from natural bentonite. It seems unlikely that the synthesised colloids would bind the radionuclides by a completely different mechanism and still have the same dissociation behaviour. Further, for the bentonite colloid samples, although the rate constants are similar to those of humic substances, the dissociation behaviour is different. Multiple first order rate constants are required to describe the dissociation of from natural organic matter (Bryan et al 2012), whilst there is clear evidence that at least some dissociation from bentonite colloids may be described with a single rate constant (e.g., Wang et al 2014; Sherriff et al 2015; Dittrich et al 2015). Therefore, it seems unlikely that entrained humic substances are responsible for the slow dissociation.

Based on the available information, it is not possible to be certain about the chemical process that is responsible for the slow dissociation. However, the behaviour seems to be unique to bentonite/montmorillonite systems. Slow dissociation of surface complexes on its own seems unlikely. Similarly, the trapping of radionuclides during the normal aggregation processes seems inconsistent with the data. In the absence of the data from Huber et al (2015), binding by entrained organic material would be a possible explanation, but the fact that synthesised montmorillonite colloids show identical behaviour suggests this is not the case.

Slow release from a common surface precipitate or gel layer is a possible explanation. Further, the behaviour seems to be particular to clay colloids, and so diffusion into the interlayer, probably accompanied by inner sphere complexation, could be taking place.

Whatever the reaction responsible for the binding of the radionuclides by the colloids, it is clear that the interaction with the bulk bentonite is quite different, for example compare the behaviour of bulk and colloidal bentonite with Eu(III) in Figure 2 and Figure 3 (also Table 1 and Table 2). The dissociation behaviour from the bulk bentonite is similar to that for humic substances, in particular the fact that there is evidence for multiple dissociation rate constants. Hence, it may be that the organic content of the clay plays a more significant role, although the other processes listed above may also play a part. In any case, data determined for bulk bentonite may not be automatically applicable to colloidal material.

4 Bentonite colloid kinetics in the safety case

4.1 An approach to assessing colloid dissociation kinetics

Whatever the chemical process responsible for the slow dissociation of radionuclides, the importance of bentonite colloids in the transport of radionuclides depends on their ability to bind radionuclides 'non-exchangeably'. The dissociation rates in Table 6 show that all of the tri and tetravalent radionuclides show broadly similar behaviour, although there is some variation in the apparent dissociation rate constant with residence/dissociation time. The rate constant controls the behaviour of the radionuclide during transport. To illustrate this, Figure 9 shows the results of transport calculations over distances of 100 m with a flow rate of 1 x 10^{-6} ms^{-1} and for residence times of 5 x 10^{-7} s in a system where the exchangeably bound metal ion is removed immediately by the rock surface and where 30% of the radionuclide is bound non-exchangeably. This calculation assumes that the colloids have no significant interaction with the rock surface. The data are plotted as the total radionuclide concentration (sorbed and in solution) versus distance from the start of the migration path as a function of the dissociation rate constant (k_b).

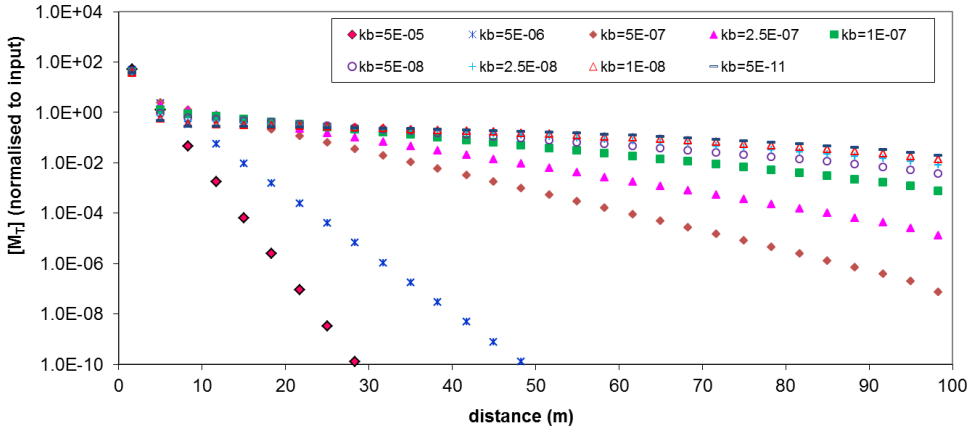

Figure 9: ***radionuclide distribution (all forms) with distance for conditions described in main text, showing the effect of radionuclide dissociation rate constant from the colloid (k_b).***

As the rate constant decreases, there is a distinct increase in the transport of the radionuclide, because it takes longer for the radionuclide to be removed from the colloid and immobilised on the rock surface. The result is that more of the radionuclide is able to travel further along the pathway.

It is also useful to consider the behaviour of the non-exchangeably bound radionuclide in isolation from the exchangeable and rock bound forms. Figure 10 shows the concentration of the non-exchangeably bound radionuclide along the transport pathway expressed as a ratio to its concentration at the start of the column. The behaviour of a conservative tracer has been plotted for comparison. As the dissociation rate constant changes, there is a steady change in the behaviour. At high values of k_b, there is little transport, because the radionuclide dissociates quickly from the colloid before it can move down the column. Eventually, when the rate constant is very high, the non-exchangeable effect will disappear, and all of the colloid bound radionuclide behaves exchangeably. As the rate constant decreases, progressively less radionuclide is able to dissociate from the colloid as it transports, with the result that the transport increases, and the behaviour tends towards that of the conservative tracer. At this point, there is no significant dissociation as the

colloid traverses the pathway, and the radionuclide has assumed the transport properties of its host colloid.

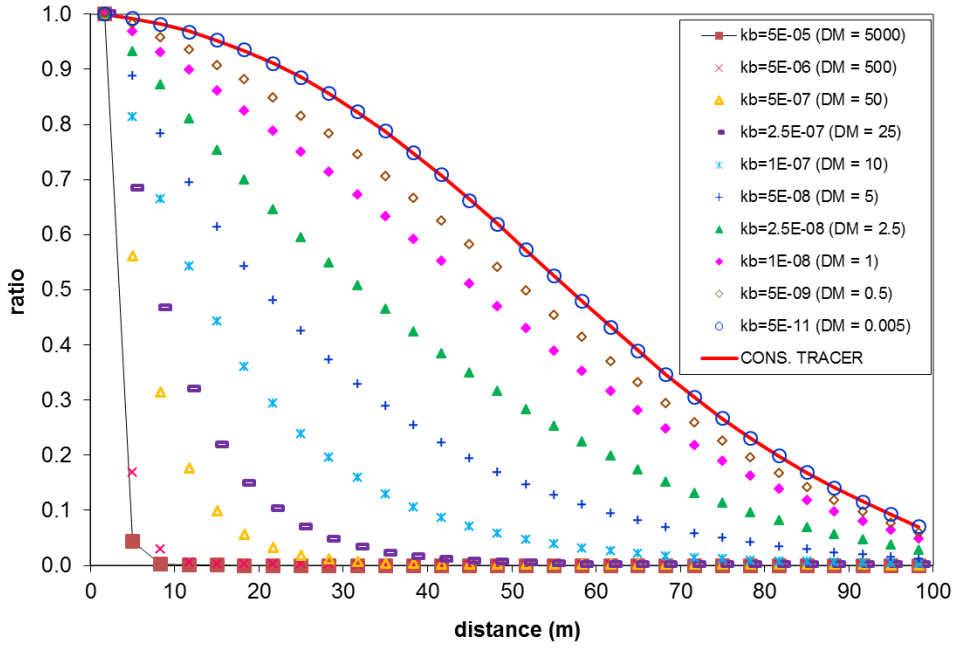

Figure 10: ***distribution of non-exchangeably bound radionuclide along the transport pathway, expressed as a ratio of its concentration at the start.***

The results of the transport calculations show that the radionuclide transport will be very sensitive to the value of the dissociation rate constant. However, the effect will depend upon the circumstances of the case: flow rate; distance; and whether the colloid itself is retarded. Therefore, a mechanism is required to predict the magnitude of the effect of the slow dissociation for a particular system. Further, transport calculations that include chemical kinetics can be computationally expensive and inconvenient and most approaches to the calculation of transport in support of safety cases assume equilibrium, often using K_d values for radionuclides. Hence, it is useful to assess whether the slow dissociation need be included in order to produce a reliable result.

In these systems, the most significant factor is whether the time that would be taken for the radionuclide to be released from the colloid is greater or less than the transport residence time, t_{res},

$$t_{res} = \frac{L}{V}$$

where L is the distance over which the transport takes place and V is the linear velocity of the mobile phase. Jennings and Kirkner (1984) found that the behaviour of a species controlled by kinetics may be rationalised using Damkohler numbers. They applied them to slow sorption onto surfaces during transport. The situation here is different, because the slow reactions involve species in the mobile phase (colloids), rather than the stationary.

We will consider a simple colloid system, with a first order dissociation rate constant, k_b, that represents a rate determining step for dissociation of radionuclides (Figure 11, inset). For such a system, it is possible to calculate the amount of radionuclide that will remain bound to the colloid with transport time relatively easily, since it will depend only on the rate constant and the time available for dissociation, which depends on the distance

travelled and the flow rate. If $[M_{non\text{-}exch}]_{t=0}$ is the concentration of non-exchangeably bound radionuclide at the start of the pathway, then the amount left after a distance, L, and a transport time, t ($[M_{non\text{-}exch}]_t$), will be given by,

$$[M_{non\text{-}exch}]_t = [M_{non\text{-}exch}]_{t=0}.e^{-tk_b}$$

Figure 11 shows the dissociation of radionuclides from colloids as a function of residence time: if the time is expressed in units of $1/k_b$, then the plot may be applied to any system. This is the basis of the Damkohler approach.

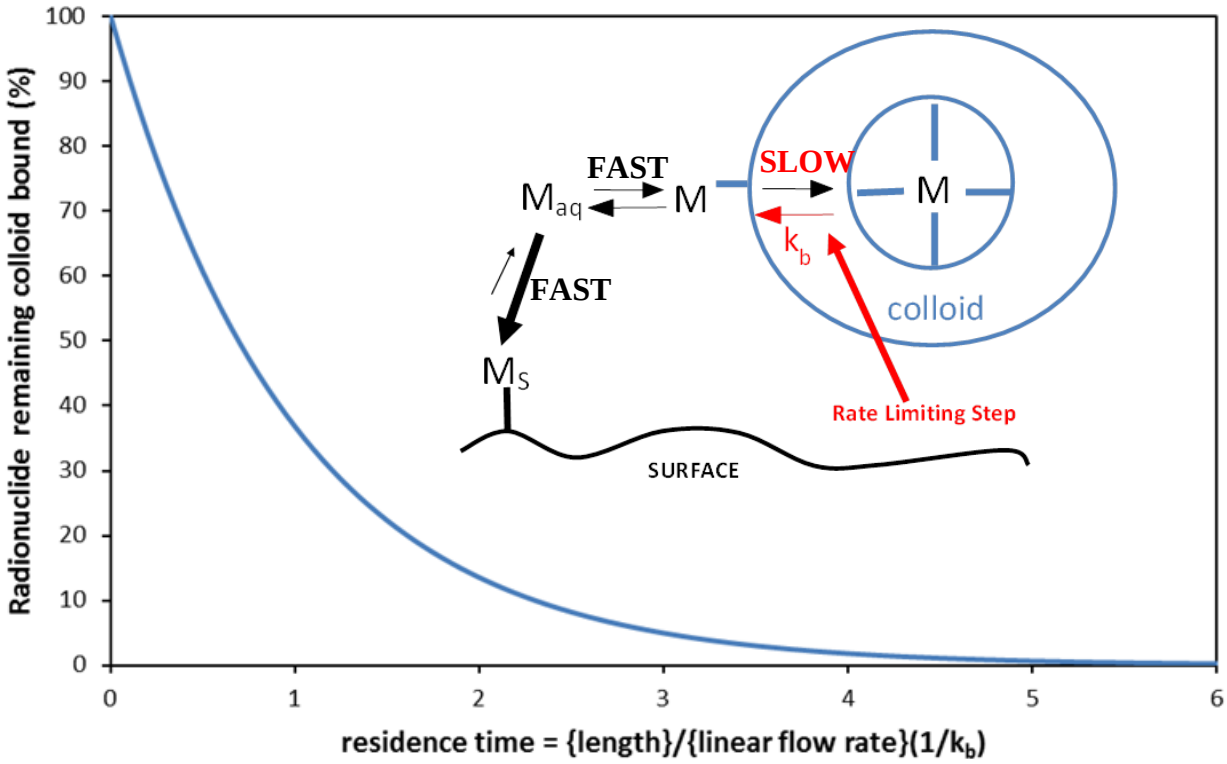

Figure 11: ***amount of radionuclide remaining colloid bound as a function of residence time, expressed as the reciprocal of the first order dissociation rate constant for a simplified colloid system with a rate limiting step for dissociation of radionuclides (M) from the colloid to allow immobilisation on the solid surface (M_S) via the free form (M_{aq}).***

The dimensionless Damkohler number for a metal ion (radionuclide) in the slowly dissociating fraction, D_M, is defined by,

$$D_M = \frac{L}{V}k_b = t_{res}k_b$$

The behaviour is controlled by the value of the dissociation rate constant, k_b, and systems with the same values of D_M will show the same behaviour, since,

$$[M_{non\text{-}exch}]_{t=t_{res}} = [M_{non\text{-}exch}]_{t=0}.e^{-t_{res}k_b} = [M_{non\text{-}exch}]_{t=0}.e^{-D_M}$$

As k_b (and so D_M) varies, there are two limiting behaviours. At high values of k_b, dissociation kinetics will be unimportant, and a simple equilibrium (e.g. K_d) approach can be used to describe the interaction of the radionuclide with the colloids. At lower k_b and D_M, kinetics will dominate the behaviour, and provided that the colloid itself is not

retarded, the behaviour of the radionuclide will tend towards that of a conservative tracer. The plots in Figure 10 have been labelled with their Damkohler number, as well as their rate constant.

The distinction between equilibrium and kinetic descriptions of chemical reactions is always artificial, since the most appropriate approach depends upon the time scale of the observation (in this case t_{res}). Given the conditions of the transport calculation, flow rate and distance, it is possible to reduce any reaction, regardless of origin or chemistry, to just three classes:

1. Those that are sufficiently fast to be treated as equilibria, i.e., high k_b and D_M;

2. Those that are sufficiently slow that they effectively do not take place (low k_b and D_M);

3. Those reactions that can only accurately be described by the use of rate equations (intermediate k_b and D_M).

Using the examples in Figure 10, the plot with $k_b = 5 \times 10^{-5}$ s^{-1} and $D_M = 5000$ shows little transport, and non-exchangeable binding has little effect. Therefore, this is a case where the transport could probably be calculated using an equilibrium (K_d) approach. At the other extreme, the plot with $k_b = 5 \times 10^{-11}$ s^{-1} and $D_M = 0.005$ shows virtually identical behaviour to that of a conservative tracer, and in this case, an adequate result would be obtained by assuming that the dissociation does not take place, i.e., the radionuclide is 'irreversibly' bound. For some other values, there is intermediate behaviour, and for example neither the assumption of equilibrium nor irreversible binding will give an accurate prediction (e.g., $k_b = 5 \times 10^{-8}$ s^{-1} and $D_M = 5$)

Therefore, we may use the limiting behaviours if D_M is sufficiently large or small. Approximations are common in complex systems, but in the case of calculations for a safety case, there is a special requirement that approximations should be conservative. Hence, whether it is appropriate to use an approximation will depend upon the application. Given that all systems with the same D_M behave in the same way, we may use it to judge the impact of dissociation kinetics, and hence to judge when it is necessary to include kinetics explicitly in transport calculations.

Decoupled Approximation

As D_M decreases, the behaviour tends towards that of a conservative tracer. In this case in the transport calculation the non-exchangeable fraction may be 'decoupled' from the remainder of the radionuclide chemistry, i.e., the reaction that connects the exchangeable and non-exchangeable may be removed from the calculation and the two fractions are treated as independent species. Beyond the fact that it reduces the mathematical complexity of the model system (and hence computing time), the advantage of this technique is that it is inherently conservative.

Equilibrium Approximation

At the other extreme of high D_M values, the behaviour of the non-exchangeable fraction tends towards that of the exchangeable. Therefore, the equilibrium approximation assumes that the non-exchangeable may be treated with the same equilibrium constant or K_d as the exchangeable. This removes the kinetics from the calculation. However, although the behaviour of the non-exchangeable does tend towards that of the exchangeable, it will always move slightly further than the exchangeable, i.e., this approximation may not be conservative. The size of the error will decrease as D_M increases. The main influence of

slow colloid dissociation kinetics is to promote migration. Therefore, any approximation that assumes that those kinetics do not exist would be expected to underestimate transport.

At intermediate values of D_M, neither the decoupled nor the equilibrium approximations will provide reliable results. To include the kinetic reaction is the only way to produce reliable predictions in this region, although this could be computationally expensive or inconvenient.

When are the Approximations Valid?

Ideally, we would like a set of rules that would allow us to decide when to use the approximations. However, that will depend upon the acceptable error and probably upon whether that error still results in a conservative prediction. The plots show that as D_M tends towards the limiting behaviours, the error introduced by using an approximation will decrease. For example, using the decoupled approximation in a system with $D_M = 0.5$ will produce a smaller error than in one with $D_M = 1$. The equilibrium approximation could be problematic, since its estimates are not conservative. The decoupled approach is always conservative, but it could lead to a significant overestimation of transport in many cases.

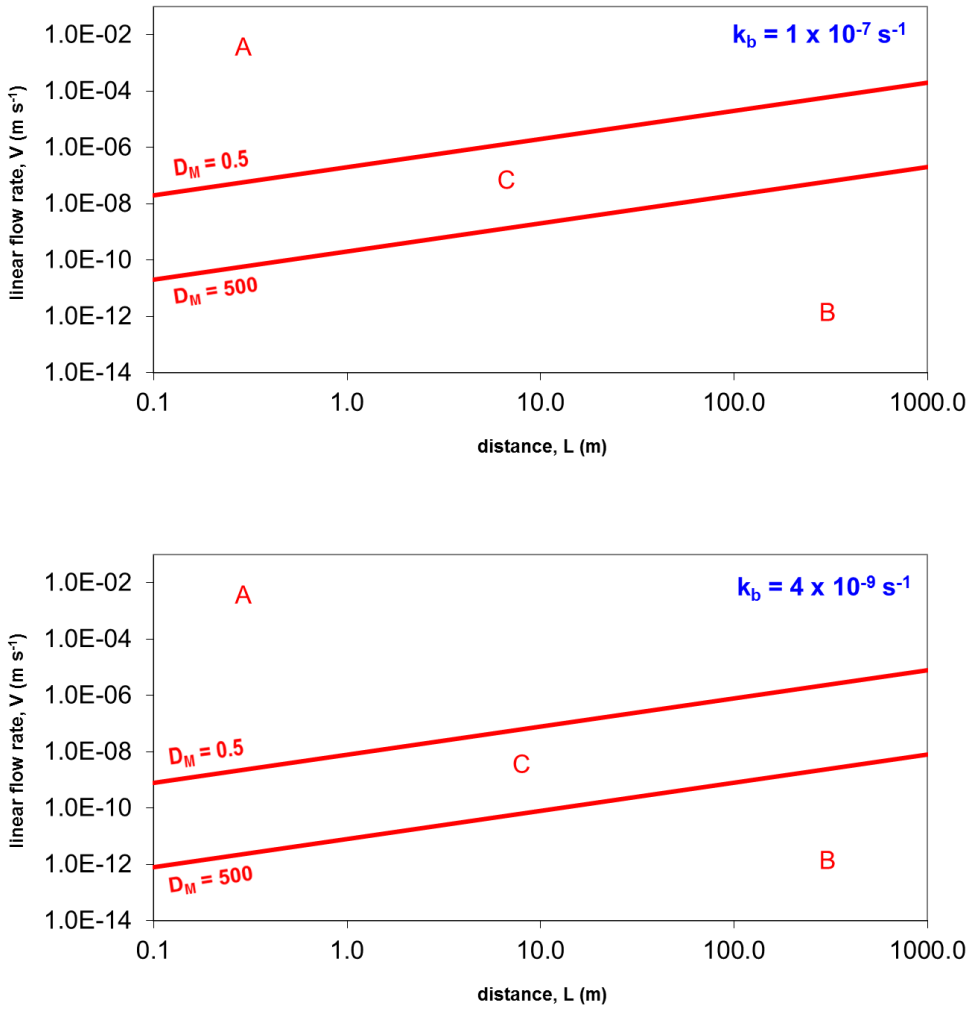

Figure 12*: Plot of linear flow rate vs distance showing the regions where the decoupled (A) and equilibrium approximations (B) might be used and where a full kinetic treatment is required (C). Upper plot $k_b = 1 \times 10^{-7}\ s^{-1}$; Lower plot $k_b = 4 \times 10^{-9}\ s^{-1}$.*

Figure 12 (linear flow rate vs distance) shows an example of this approach: the area is divided into three regions. In region A, the decoupled approximation is appropriate, but moving down and right, the error introduced with the decoupled approximation will get larger (although the prediction will always be conservative). In the bottom right hand corner (region B): the equilibrium approximation will be more appropriate, although moving up and to the left, the error incurred will become larger, and this time it will not be conservative. In region C, a full treatment of kinetics is best. The arbitrary limits in the figure are based and D_M boundaries of 0.5 for the decoupled and 500 for the equilibrium approximations. Plots have been given for dissociation rate constants of 1 x 10^{-7} s^{-1} and also for 4 x 10^{-9} s^{-1}, since the data of Huber et al (2015), which have the longest reaction times, suggest values of the order of 10^{-7} s^{-1} are appropriate, whilst the extrapolations of the experimental data (Figure 7; **Error! Reference source not found.**) suggest that lower rate constants of the order of 4 x 10^{-9} s^{-1} may be more appropriate at longer residence times. Note, the appropriate limiting values of D_M will depend upon the application.

4.2 Calculations including the sorption/instability of colloids

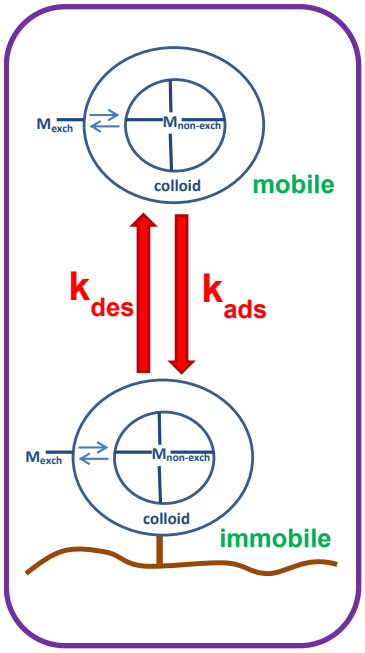

Figure 13: ***removal of radionuclide carrying colloids from solution***

The Damkohler treatment thus far has taken no account of the sorption of colloids during transport or colloid instability. Colloid sorption and instability are complex processes and both could be slow. For the purposes of the following analysis, we will combine all processes that could remove colloids (and hence the radionuclides associated with them) into a single combined reaction linking colloids in solution, $Coll_{mobile}$, with those removed from solution by any process, $Coll_{immobile}$ (Figure 13),

$$Coll_{mobile} \rightleftarrows Coll_{immobile}$$

Transfer between the fractions is described with a rate equation,

$$\frac{d[Coll_{immobile}]}{dt} = k_{ads}[Coll_{mobile}] - k_{des}[Coll_{immobile}]$$

where k_{ads} and k_{des} are the first order rate constants for transfer out of and back into solution, respectively. Any colloid bound radionuclides will be affected by the same rate constants. In the case of the interaction of the radionuclides with the colloids, it is only the dissociation rate constant (k_b) that makes a significant difference to the transport. Here, the forward and backward rate constants could be significant.

Radionuclide behaviour in a system with both colloid sorption/instability and slow dissociation of radionuclide from the colloid is harder to rationalise than systems where colloids transport conservatively, or with independent kinetic processes, because here they interact. The rate of the colloid removal process affects the residence time of the colloid in the groundwater, and hence the relative effect of the radionuclide dissociation rate. However, we can define a Damkohler number for the colloid removal process, D_C,

$$D_C = \frac{k_{ads}}{V} L$$

As D_C approaches zero, the behaviour of the colloid (and any associated radionuclide) will tend towards that of a conservative tracer, whilst as D_C tends to infinity, the extent of sorption will increase, and tend towards equilibrium behaviour, in which case the amount of colloid removed from solution at any point and time is given by,

$$[Coll_{immobile}] = K_C [Coll_{mobile}]$$

where,

$$K_C = \frac{k_{ads}}{k_{des}}$$

As for the interaction of the radionuclide with the colloid, at the upper and lower limits, a kinetic calculation may be avoided by assuming that the colloid complex either:

1. does not sorb at all, and so transports with the velocity of the groundwater (low D_C);

2. or that it does sorb, and that the interaction may be described with an equilibrium constant, K_C (high D_C).

Assuming that the colloid does not sorb will give a conservative prediction, whilst the equilibrium approach may not, since the equilibrium assumption produces the maximum possible retardation, and the real behaviour only tends to this as D_C increases. At intermediate values, only a full kinetic description will provide an accurate prediction.

If a colloid with an associated radionuclide is removed from solution, then that in itself will cause some retardation. However, it will also increase the residence time of the complex in the water column, allowing more time for dissociation of the radionuclide and immobilisation on the rock surface (Figure 14). Hence, the effective residence time is now greater than that of the solution.

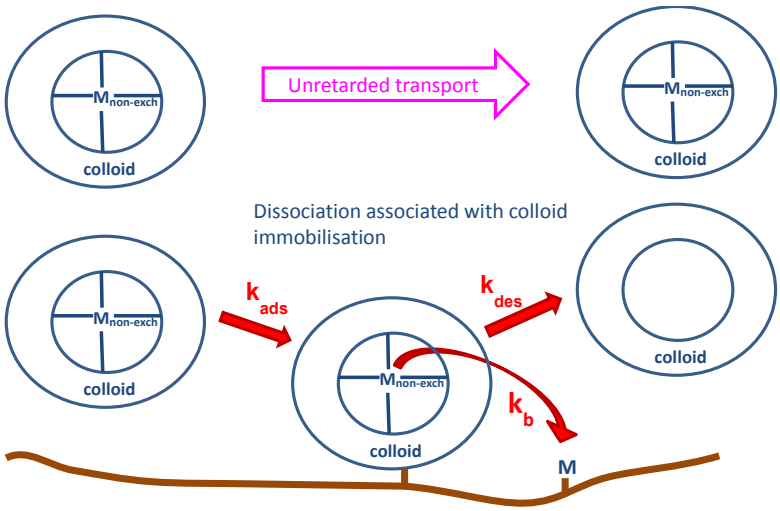

Figure 14: ***effect of colloid sorption /instability on radionuclide dissociation*****.**

The extent of this effect will depend upon the affinity of the complex for the surface and the colloid Damkohler number (D_C). If D_C is small, then the residence time is too short for removal from solution to be significant, the complex transports with the velocity of the groundwater, and there is no effect upon the radionuclide-colloid kinetics, i.e. the behaviour of the metal is still controlled solely by k_b, and D_M may still be used to define the behaviour of the radionuclide,

$$D_M = \frac{k_b}{V} L \Big|_{D_C \to 0}$$

However, in the case of significant retardation of the colloid, the Damkohler number for the slowly dissociating radionuclide must be adapted to take account of the increased residence time. If D_C is large ($D_C \to \infty$), and the colloid removal process may be described with an equilibrium constant, K_C, then the effective metal ion Damkohler number, D_M^{eff}, will be given by,

$$D_M^{eff} = \frac{k_b}{V} L (1 + K_C) \Big|_{D_C \to \infty}$$

For systems with intermediate values of D_C, these equations may be used to provide a range of Damkohler numbers, the most representative value lying in between.

To assess the importance of slow dissociation kinetics in a system that includes colloid immobilisation processes and to determine the most appropriate approximations, first D_C should be calculated. If it is small, then D_M may be used to determine whether slow dissociation kinetics are significant, whilst if it is large, D_M^{eff} should be used. If D_C has an intermediate value, then D_M will provide an indication of the maximum possible effect of slow dissociation and D_M^{eff} the minimum. Figure 15 shows the procedure that should be used for selecting the most appropriate approximations if any, to describe slow dissociation and colloid removal processes. MAX1 and MIN1 are the Damkohler number limits for the colloid removal, i.e.: if D_C < MIN1, then colloid sorption could be ignored; if D_C > MAX1, then it would be included using an equilibrium constant; if MIN1 < D_C < MAX1, then the full rate equation would be used. Similarly, MAX2 and MIN2 are the limits for determining the approach to calculating the slow dissociation of radionuclides from colloids. These values would depend upon the requirements of the calculation and the acceptable errors. Depending upon D_C and D_M or D_M^{eff}, there are 9 possible options, 5 of

which are conservative and 4 non-conservative. 4 of the options avoid all kinetic equations, another 4 include 1 kinetic process, and only one option requires a kinetic description of both colloid removal and slow dissociation. Of course, the exact solution with a kinetic description of both processes will always give the correct solution.

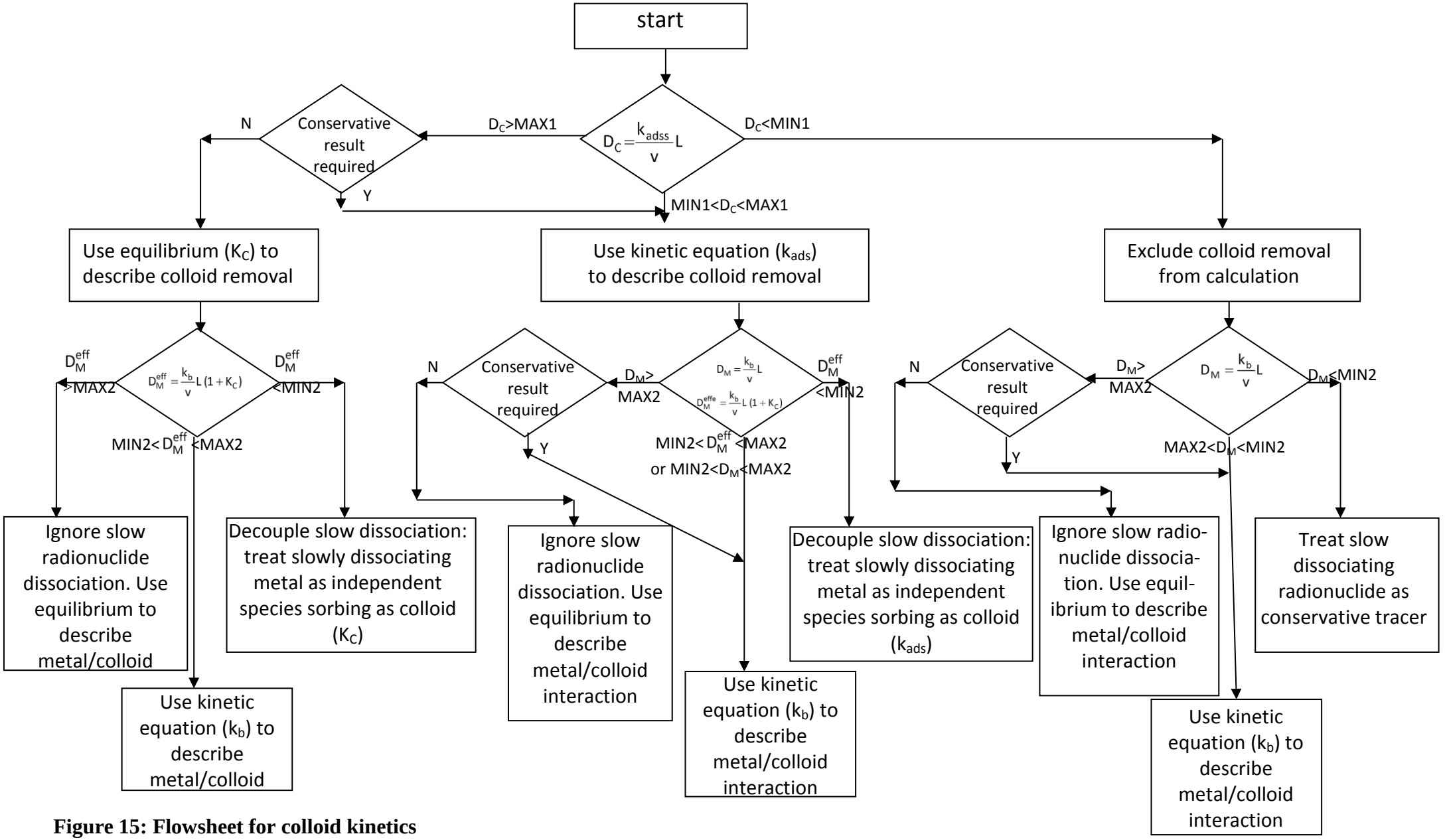

Figure 15: Flowsheet for colloid kinetics

4.3 Estimates of radionuclide transport

Taking into account all of the available experimental data (Table 6), we can be realtively confident of the appropriate dissociation rate constants for residence times up to approximately 1 year. The data of Huber et al (2015) have the longest dissociation reaction time (approximately 400 days). They are also consistent with the values for the other batch and column experiments. They show that dissociation rate constants of the order of 10^{-7} s^{-1} are likely for tri and tetravalent ions. Hence, this value serves as an upper bound for the most appropriate to use in transport calculations.

For residence times beyond 1 year, the situation becomes progressively less clear as the residence time increases. Extrapolation of the experimental data for longer reaction times suggests that values of the order of 4 x 10^{-9} s^{-1} might be observed at very long residence times, although that value comes with a large *caveat*, and it is possible that some fraction of colloid bound radionuclides might show even slower dissociation. Alternatively, it is also possible that 10^{-7} s^{-1} represents the most appropriate value under all conditions. Hence, the behaviour of a system with $k_b = 10^{-7}$ s^{-1} is certainly of interest, and it is sensible to consider at least a system with $k_b = 4 \times 10^{-9}$ s^{-1}.

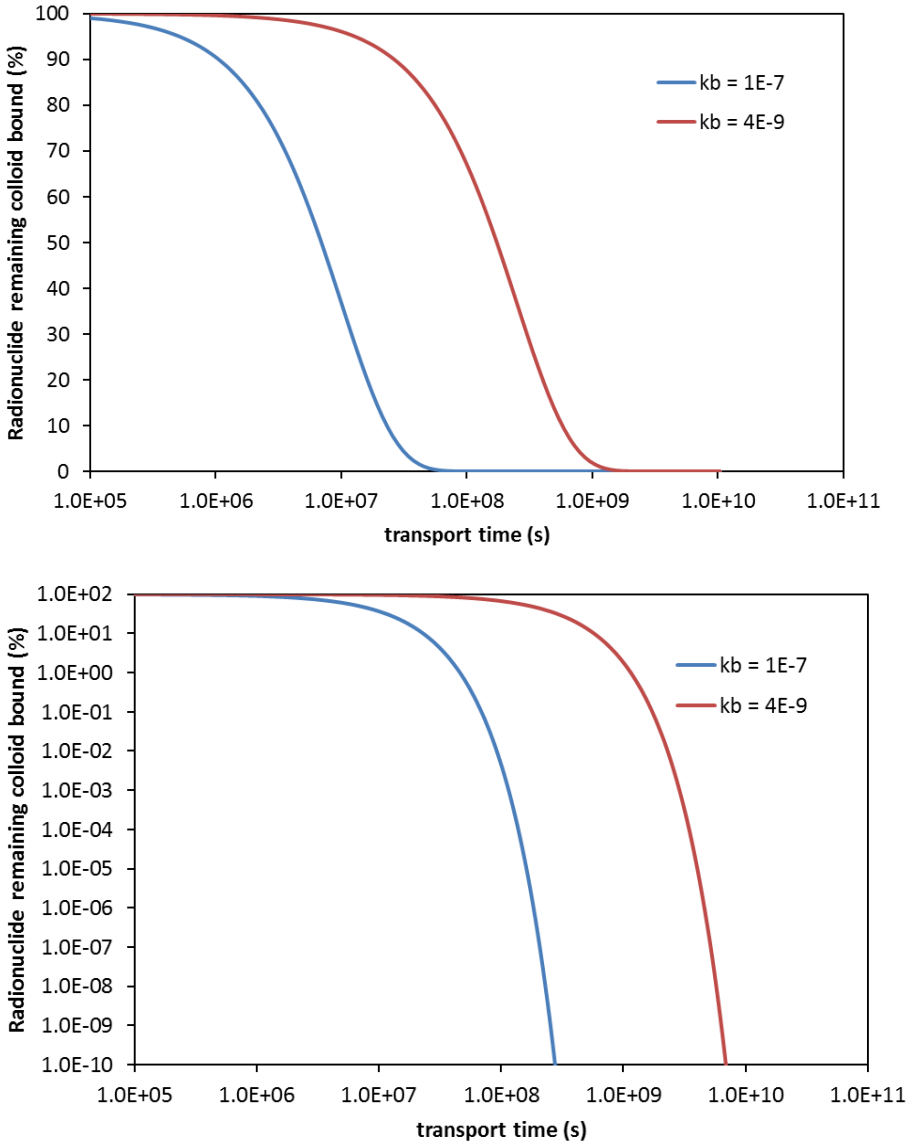

Figure 16: ***percentage of radionuclide remaining colloid bound versus time from the start of transport for $k_b = 1 \times 10^{-7}$ s^{-1} and 4×10^{-9} s^{-1}; upper linear vertical scale; lower same data with log scale.***

Figure 16 shows the amount of non-exchangeably bound radionuclide that would be expected to remain bound to bentonite colloids plotted against the time since the start of their transport. Plots are given for $k_b = 1 \times 10^{-7}$ s^{-1} and 4×10^{-9} s^{-1} (the data have been given on linear and log scales). Given the currently available knowledge, and rembering the *caveat* given above, we would expect the behaviour of the radionuclide to fall somewhere between the plots for the two rate constants.

The advantage of plotting the amount of radionuclide remaining bound to the colloid against time since the start of transport is that the plots are correct for systems with or without retardation of the colloid. Further, for systems where there is no colloid retardation, then the vertical scale is also equivalent to the amount of radionuclide remaining in the mobile phase.

Figure 17 - Figure 20 show the amount that would be expected to remain in the mobile phase as distance from the start of the pathway increases for linear flow rates from 10^{-5} ms^{-1} to 10^{-8} ms^{-1}. This time, the data are only valid for a system where there is no significant retardation of the bentonite colloids themselves. Any colloid sorption would shift the plots towards the left (less radionuclide transport).

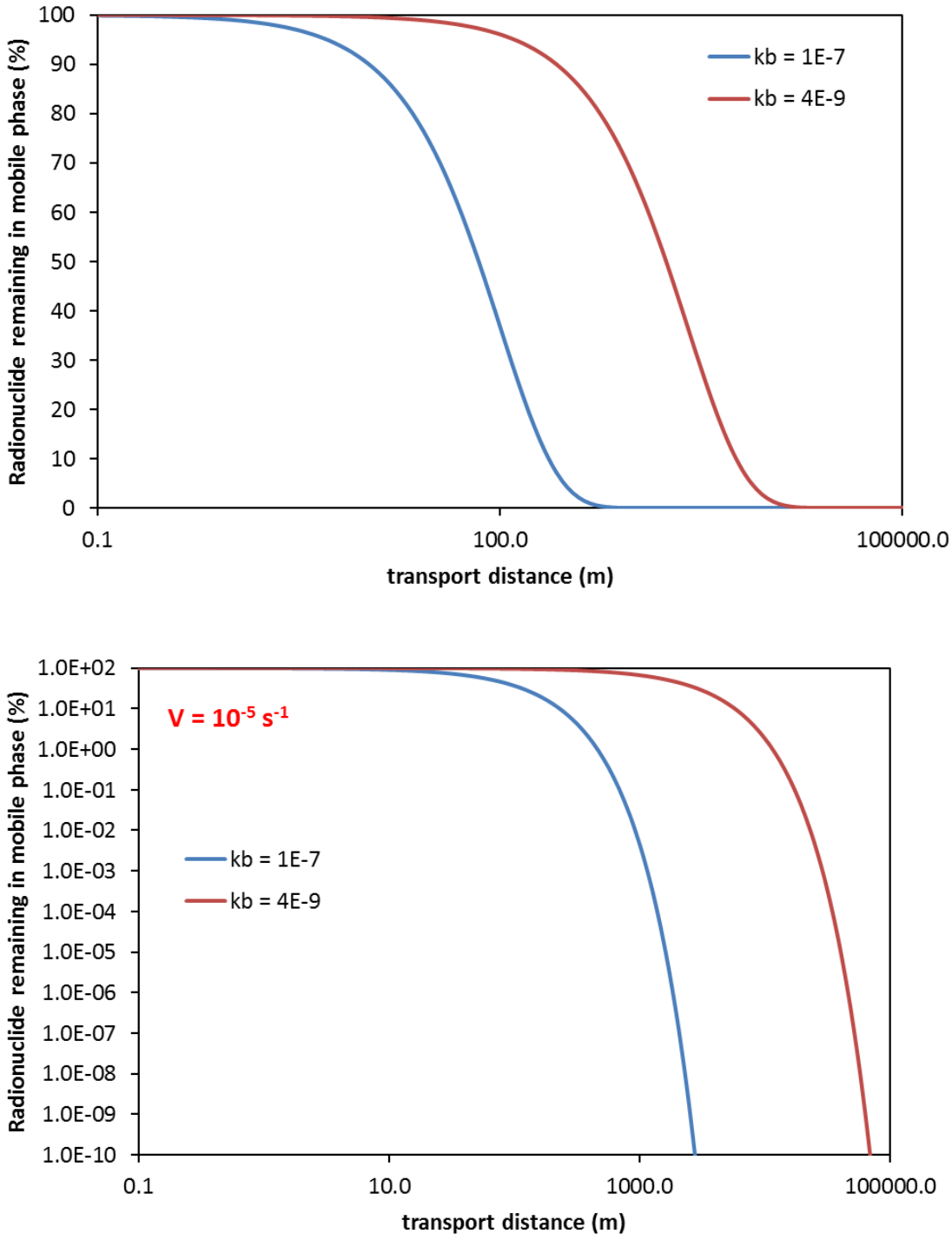

Figure 17: ***percentage of radionuclide remaining in the mobile phase versus distance for a flow rate of 10^{-5} ms^{-1} and for k_b = 1 x 10^{-7} s^{-1} and 4 x 10^{-9} s^{-1}; upper linear vertical scale; lower same data with log scale.***

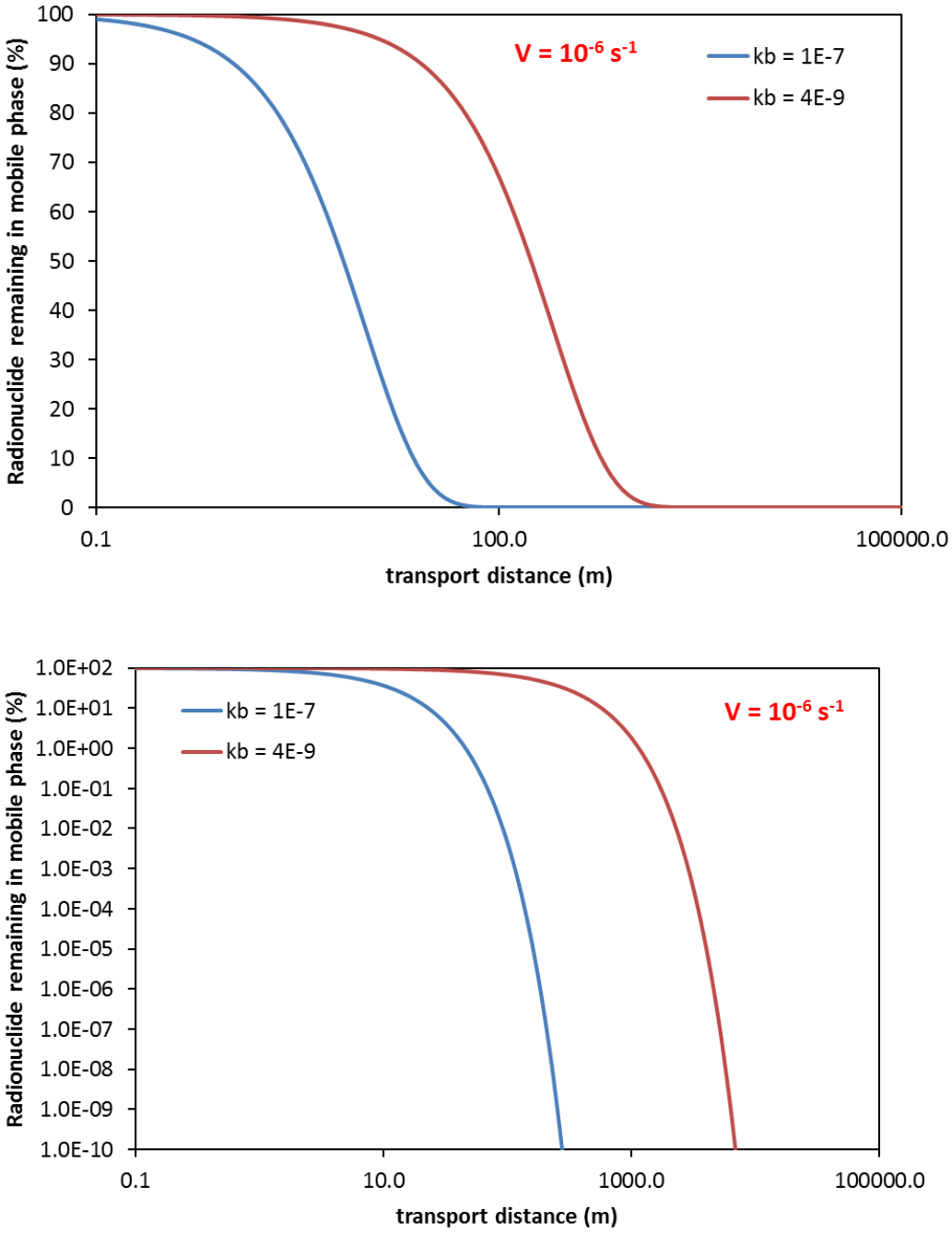

Figure 18: ***percentage of radionuclide remaining in the mobile phase versus distance for a flow rate of 10^{-6} ms^{-1} and for k_b = 1 x 10^{-7} s^{-1} and 4 x 10^{-9} s^{-1}; upper linear vertical scale; lower same data with log scale.***

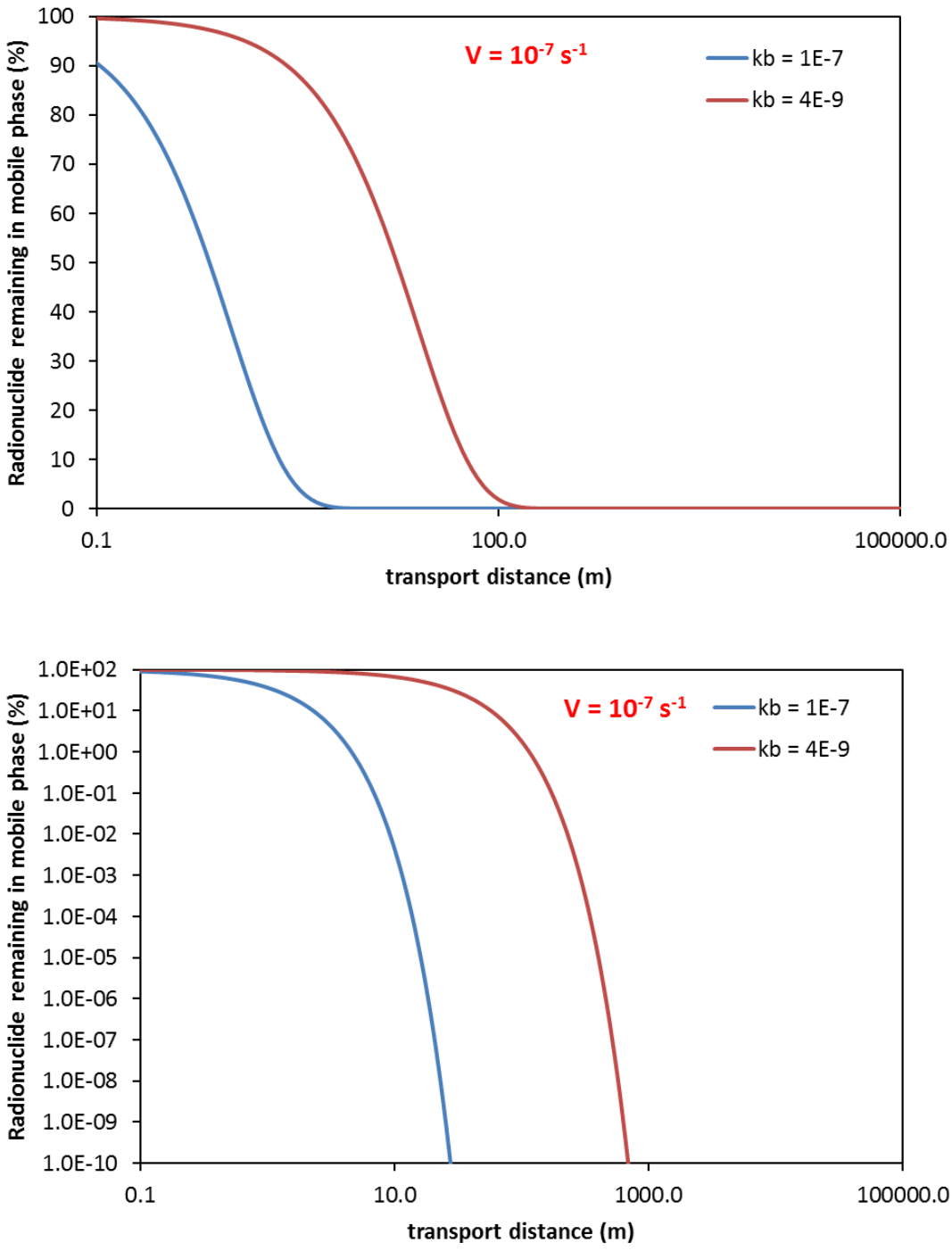

Figure 19: ***percentage of radionuclide remaining in the mobile phase versus distance for a flow rate of 10^{-7} ms^{-1} and for k_b = 1 x 10^{-7} s^{-1} and 4 x 10^{-9} s^{-1}; upper linear vertical scale; lower same data with log scale.***

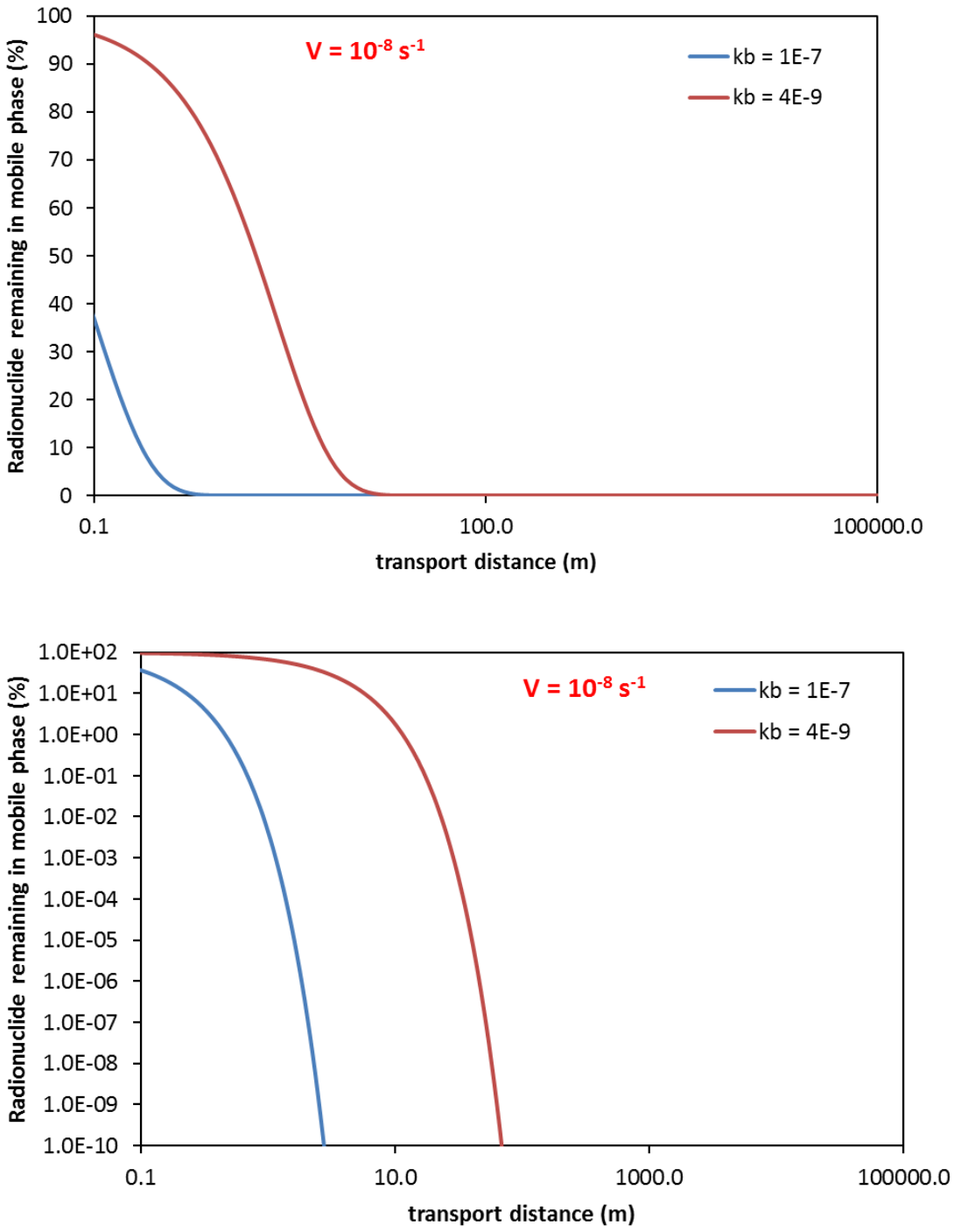

Figure 20: ***percentage of radionuclide remaining in the mobile phase versus distance for a flow rate of 10^{-8} ms^{-1} and for k_b = 1 x 10^{-7} s^{-1} and 4 x 10^{-9} s^{-1}; upper linear vertical scale; lower same data with log scale.***

5 Conclusions

Over the last 5 years, there has been a significant increase in the understanding of radionuclide interactions with bentonite colloids. A number of new dissociation data sets have been produced. Further, it has been shown that the behaviours observed by different groups using different techniques and for different elements are all consistent.

For situations in the laboratory or the environment where the colloid residence time is of the order of one year or less, then the most appropriate rate constant to use for transport calculations is of the order of 10^{-7} s^{-1} for both the tri and tetravalent elements. Based on all of the available data, for situations where the residence time is greater than 1 year, then the value of 10^{-7} s^{-1} represents an upper limit for the most appropriate value. Extrapolation of the experimental data, suggests that the rate constants of as low as 4×10^{-9} s^{-1} may be appropriate, although there is some considerable uncertainty, and whilst it is possible that some fraction of the non-exchangeably bound radionuclides dissociate with rate constants that are even lower than this value, at the same time it is also possible that the value of 10^{-7} s^{-1} is appropriate under all conditions.

Significantly, although the existence of a small fraction of bound radionuclides that are (pseudo-) 'irreversibly' bound cannot be excluded, in none of the experiments to date has there been definitive evidence for the existence of such a fraction. Further, the amount of any radionuclide bound irreversibly must be a small fraction of the total.

A procedure based on Damkohler numbers may be used to assess the likely impact of slow dissociation kinetics on radionuclide transport. This may be used with the range of rate constants from the experiments.

Mori et al (2003) developed the so called 'Colloid Ladder'. Taking into account the work reported here, an adapted version is shown in Figure 21. The original final criterion was 'is uptake irreversible?'. However, it has become clear that slow dissociation short of irreversibility can promote some transport. Radionuclides will be transported provided that the time required for them to dissociate from the colloid is of the same order or greater than the transport residence time. Hence, a dissociation rate constant that made a significant difference to radionuclide transport in one case, might be much less important in a different scenario, for example at a slower flow rate.

Therefore, whether or not slow colloid dissociation kinetics will have an impact will vary from case to case. However, using the rate data and Damkohler method described here, it is possible to determine their likely effect and whether the kinetics need to be considered explicitly on a case by case basis.

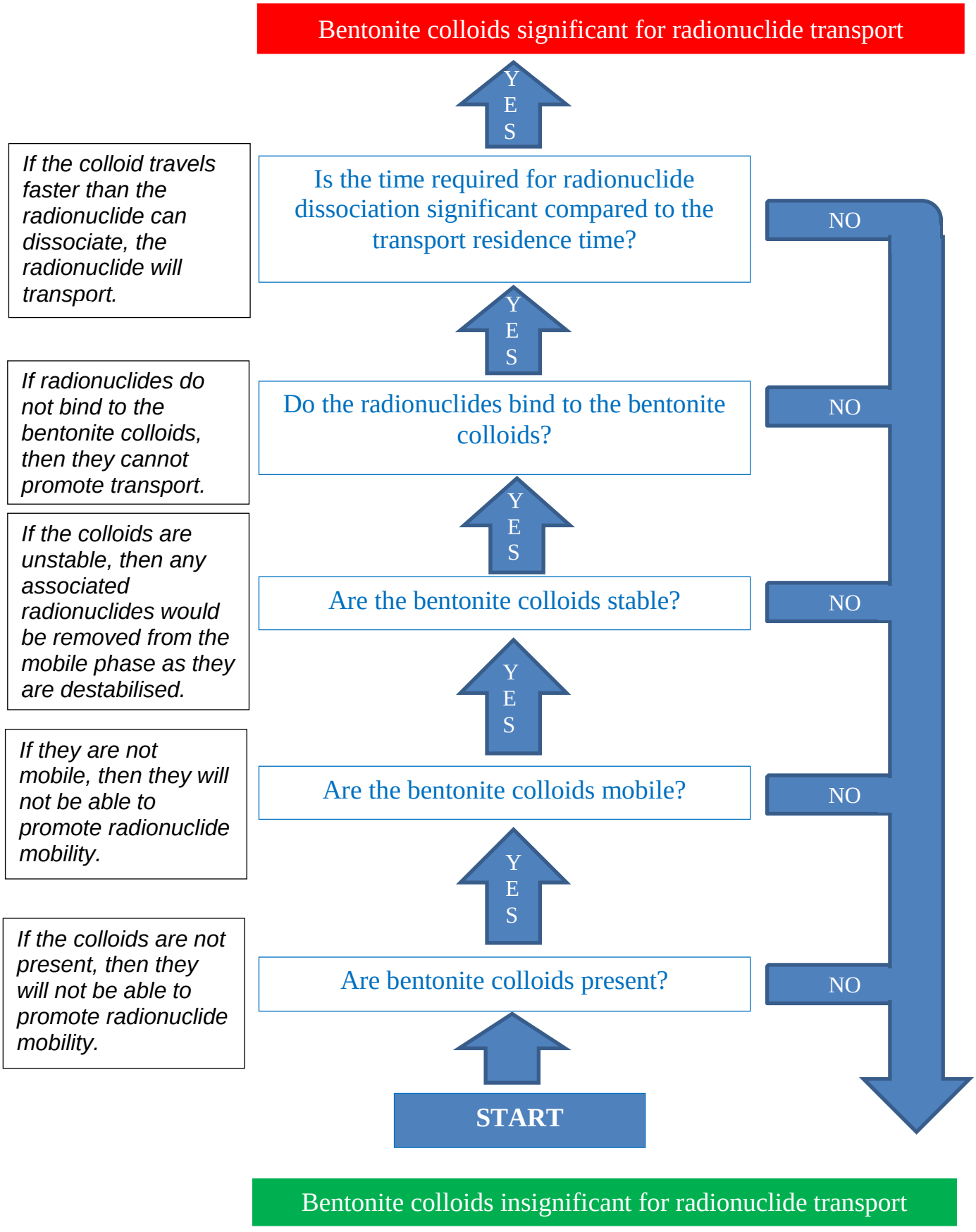

Figure 21: ***The amended colloid ladder taking into account the results of BELBaR.***

Acknowledgements

The author would like to thank all of those that have contributed to the experimental and modelling work that is reviewed in this report and the European Union for funding this work through the BELBaR project.

References

M. Bouby, H. Geckeis, J. Lutzenkirchen, S. Mihai, T. Schafer, 2011, Interaction of bentonite colloids with Cs, Eu, Th and U in presence of humic acid: A flow field-flow fractionation study, Geochimica et Cosmochimica Acta, 75, 3866–3880.

F. Brandberg, K. Skagius, 1991, Porosity, sorption and diffusivity data compiled for the SKB 91 study, SKB Report 91-16, 1991

N.D. Bryan, L. Abrahamsen, N. Evans, P. Warwick, G. Buckau, L.P. Weng and W.H. Van Riemsdijk, 2012, The effects of humic substances on the transport of radionuclides: Recent improvements in the prediction of behaviour and the understanding of mechanisms. Applied Geochemistry, 27, 378-389.

T.M. Dittrich, H. Boukhalfa, S.D. Ware, P.W. Reimus, 2015, Laboratory investigation of the role of desorption kinetics on americium transport associated with bentonite colloids, Journal of Environmental Radioactivity, 148, 170-182.

H. Geckeis, T. Schäfer, W. Hauser, T. Rabung, T. Missana, C. Degueldre, A. Möri, J. Eikenberg, T. Fierz, W.R. Alexander, 2004, Results of the Colloid and Radionuclide Retention experiment (CRR) at the Grimsel Test Site (GTS), Switzerland -Impact of reaction kinetics and speciation on radionuclide migration. Radiochimica Acta. 92, 765-774.

B.D. Honeyman, 1999, Colloidal culprits in contamination. Nature, 397, 23–24.

F. Huber, P. Kunze, H. Geckeis, T. Schäfer, 2011, Sorption reversibility kinetics in the ternary system radionuclide-bentonite colloids/nanoparticles-granite fracture filling material. Applied Geochemistry, 26, 2226–2237.

F.M.Huber, S. Heck, L. Truche, M. Bouby, J. Brendle, P. Hoess, T. Schäfer, 2015, Radionuclide desorption kinetics on synthetic Zn/Ni-labelled montmorillonite nanoparticles, Geochimica et Cosmochimica Acta, 148, 426–441.

A.A. Jennings and D.J. Kirkner, 1984, Instantaneous equilibrium approximation analysis. Journal of Hydraulic Engineering (A.S.C.E.), 110, 1700 – 1717.

W. Miller, R. Alexander, N. Chapman, I. McKinley, J. Smellie, 1994, Natural analogue studies in the geological disposal of radioactive waste. Studies in Environmental Science, 57.

T. Missana, Ú. Alonso, M. García-Gutiérrez, and M. Mingarro, 2008, Role of bentonite colloids on europium and plutonium migration in a granite fracture. Applied Geochemistry, 23, 1484-1497.

A. Möri, W.R. Alexander, H. Geckeis, W. Hauser, T. Schäfer, J. Eikenberg, T. Fierz, C. Degueldre, T. Missana, 2003, The colloid and radionuclide retardation experiment at the Grimsel Test Site: influence of bentonite colloids on radionuclide migration in a fractured rock. Colloids and Surfaces A: Physicochemical and Engineering Aspects, 217, 33-47.

J.N. Ryan, M. Elimelech, 1996, Review: colloid mobilization and transport in groundwater. Colloid Surface A, 107, 1–56.

N. Sherriff, R. Issa, K. Morris, F. Livens, S. Heath N. Bryan, 2015, Reversibility in radionuclide/bentonite bulk and colloidal ternary systems, Mineralogical Magazine, 79, 1307-1315.

N. Sherriff, F. Livens, N. Bryan, O. Elo, N. Huittinen, K. Müller, P. Hölttä, U. Alonso, T. Missana, 2015b, Understanding of Radionuclide Colloid Interaction (with special emphasis on sorption reversibility), BELBaR report D3.9, 2015.

Y. Wang, E. Matteo, J. Rutqvist, J. Davis, L. Zheng, J. Houseworth, J. Birkholzer, T. Dittrich, C.W. Gable, S. Karra, N. Makedonska, S. Chu, D. Harp, S.L. Painter, P. Reimus, F. Perry, P. Zhao, J. Begg, M. Zavarin, S.J. Tumey, Z. Dai, A.B. Kersting, J. Jerden, K. Frey, J.M. Copple, W. Ebert, 2014, Used Fuel Disposal in Crystalline Rocks: Status and FY14 Progress, FCRD-UFD-2014-000060, September 26, 2014.

S. Wold, 2010, Sorption of prioritized elements on montmorillonite colloids and their potential to transport radionuclides, SKB Technical Report, TR-10-20.